

2025

The effects of norepinephrine ablation on behavior during a probabilistic switching task in male and female mice

<https://hdl.handle.net/2144/52410>

"Downloaded from OpenBU. Boston University's institutional repository."

BOSTON UNIVERSITY

ARAM V. CHOBANIAN & EDWARD AVEDISIAN SCHOOL OF MEDICINE

Thesis

**THE EFFECTS OF NOREPINEPHRINE ABLATION ON BEHAVIOR DURING
A PROBABILISTIC SWITCHING TASK IN MALE AND FEMALE MICE**

by

SELIN YALCIN

B.S., Stony Brook University, 2022

Submitted in partial fulfillment of the

requirements for the degree of

Master of Science

2025

Approved by

First Reader

Michael Wallace, Ph.D.
Assistant Professor of Anatomy and Neurobiology

Second Reader

Jean-Jacques Soghomonian, Ph.D.
Associate Professor of Anatomy and Neurobiology

Third Reader

Lynne Chantranupong, Ph.D.
Assistant Professor of Biology

ACKNOWLEDGMENTS

I would like to express my heartfelt gratitude to all those who have supported me throughout the journey of this project. First and foremost, I am grateful to Dr. Wallace, my supervisor, for his guidance, wisdom, and encouragement. His insights and constant support have been invaluable throughout this process. A special thanks to Dr. Joseph Martinez for providing the inspiration and motivation that helped shape my ideas and keep me focused.

I would also like to thank my lab colleagues and peers, for their collaboration, constructive feedback, and camaraderie during this project. Your perspectives and knowledge have contributed greatly to my work.

Finally, I would like to thank my family and friends for their encouragement. Their belief in me has been a constant source of strength, and I couldn't have completed this without their support.

**THE EFFECTS OF NOREPINEPHRINE ABLATION ON BEHAVIOR DURING
A PROBABILISTIC SWITCHING TASK IN MALE AND FEMALE MICE**

SELIN YALCIN

ABSTRACT

The process of selecting an action, assessing it, and storing the outcome to guide future responses involves the basal ganglia and extended circuits like the Lateral Habenula. Activity in the Lateral Habenula is observed in various human neurological disorders where action selection is impaired. Additionally, the Lateral Habenula likely functions as a key hub for the interaction between stress and decision-making. Elevated levels of norepinephrine, which originates in the locus coeruleus, are a hallmark of the stress response and serve as signaling molecules in the brain. In the Lateral Habenula, norepinephrine is known to play a role in both arousal and anxiety states. However, the precise mechanisms underlying the Lateral Habenula's function and its interaction with norepinephrine during action evaluation are not yet fully understood. Gaining insight into Lateral Habenula function in action selection is crucial for understanding how disruptions in these circuits contribute to dysfunction and disease. A variation of the two-armed bandit behavioral task that allows for the manipulation and observation of norepinephrine circuit dynamics in vivo during a thirst-motivated was used to determine if norepinephrine signaling is necessary for port switching and retention of the task due to its role in attention allocation and working memory. The study demonstrated some changes; however, the results would likely become more pronounced with larger sample sizes, which could enhance the statistical power and precision of the findings.

TABLE OF CONTENTS

ACKNOWLEDGMENTS	iv
ABSTRACT.....	v
TABLE OF CONTENTS.....	vi
LIST OF TABLES	viii
LIST OF FIGURES	ix
LIST OF ILLUSTRATIONS	xi
LIST OF ABBREVIATIONS.....	xii
INTRODUCTION	1
Locus Coeruleus	1
Norepinephrine	4
Lateral Habenula.....	6
Reward Prediction.....	8
DSP-4.....	8
Behavioral Task	9
Hypothesis	10
MATERIALS AND METHODS.....	12
Experimental Subjects	12
Injections.....	12
Behavior Apparatus and Training.....	14
Immunohistochemistry Protocol.....	17
RESULTS	19

90-10	19
Male vs Female 90-10.....	27
70-30	35
Male vs Female 70-30.....	39
Immunohistochemistry	47
DISCUSSION	50
APPENDIX.....	52
BIBLIOGRAPHY.....	54
CURRICULUM VITAE.....	57

LIST OF TABLES

Table 1.	14
---------------	----

LIST OF FIGURES

Figure 1	3
Figure 2	20
Figure 3	21
Figure 4	22
Figure 5	23
Figure 6	24
Figure 7	25
Figure 8	26
Figure 9	27
Figure 10	28
Figure 11	29
Figure 12	30
Figure 13	31
Figure 14	32
Figure 15	33
Figure 16	34
Figure 17	35
Figure 18	36
Figure 19	37
Figure 20	38
Figure 21	39

Figure 22	40
Figure 23	41
Figure 24	42
Figure 25	43
Figure 26	44
Figure 27	45
Figure 28	46
Figure 29	47
Figure 30	48
Figure 31	49
Supplemental Figure 1	52
Supplemental Figure 2	52
Supplemental Figure 3	53

LIST OF ILLUSTRATIONS

Illustration 1	7
Illustration 2	11
Illustration 3	16

LIST OF ABBREVIATIONS

2ABT.....	2 Armed Bandit Task
BU.....	Boston University
DSP-4.....	N-(2-chloroethyl)-N-ethyl-2-bromobenzylamine
LC	Locus Coeruleus
LHb	Lateral Habenula
MHb	Medial Habenula
NE.....	Norepinephrine
NET.....	Norepinephrine Transporter
TH.....	Tyrosine Hydroxylase

INTRODUCTION

Locus Coeruleus

The locus coeruleus (LC), which translates from Latin as "blue spot," is a small, evolutionarily conserved nucleus situated deep within the brainstem. It is the main source for noradrenaline the brain's widespread norepinephrine neurotransmitter system (Poe et al., 2020). Previously the LC was believed to be composed of a compact group of relatively uniform neurons located in the dorsal pons of the brainstem (Palkovits et al, 1983) but more recent studies have shown that LC neurons can be categorized electrophysiologically into two subclasses (Tortorelli et al, 2022). Due to its deep location and small size (~3000 neurons Sara 2009), studying LC neuronal activity and linking it to environmental events and behavior has been challenging. However, recent advancements in neuroscience have provided unprecedented access to this elusive nucleus, uncovering new insights into its organization and function.

For more than five decades, the LC was believed to be homogeneous in both structure and function, with its primary neurotransmitter, norepinephrine (NE), being released uniformly to influence cells and circuits across the forebrain, brainstem, cerebellum, and spinal cord. Given the LC's projections to many areas of the central nervous system with diverse functions, researchers have traditionally viewed the locus coeruleus-norepinephrine (LC-NE) system as a unified force acting on neural networks and behavior (Palkovits et al, 1983, Figure 1). However, what was thought to be known about the widely projecting efferent and convergent afferent anatomy of these neurons was inaccurate. Instead, the distribution of LC-NE axonal fibers is nonuniform across the

neocortex (Berridge et al., 2003). The LC is reported to receive input from up to 111 different brain regions, including most areas of the brainstem and forebrain (Breton-Provencher et al., 2021, Figure 1). Notably, brainstem inputs, especially from the giant cellular reticular nucleus, which responds to tactile, visual, vestibular, and olfactory stimuli, lead to LC activation in response to salient sensory information (Tabansky et al., 2018). At the same time, top-down inputs from the prefrontal cortex (PFC) and central amygdala can influence the intensity of LC activation (Tabansky et al., 2018, Figure 1). These converging inputs suggest the LC is involved in both bottom-up sensory-driven and top-down goal-directed regulation of behavior (Breton-Provencher et al., 2021). This input-output structure allows the LC to modulate brain function in response to external stimuli and internal states, and to shape this function through learning.

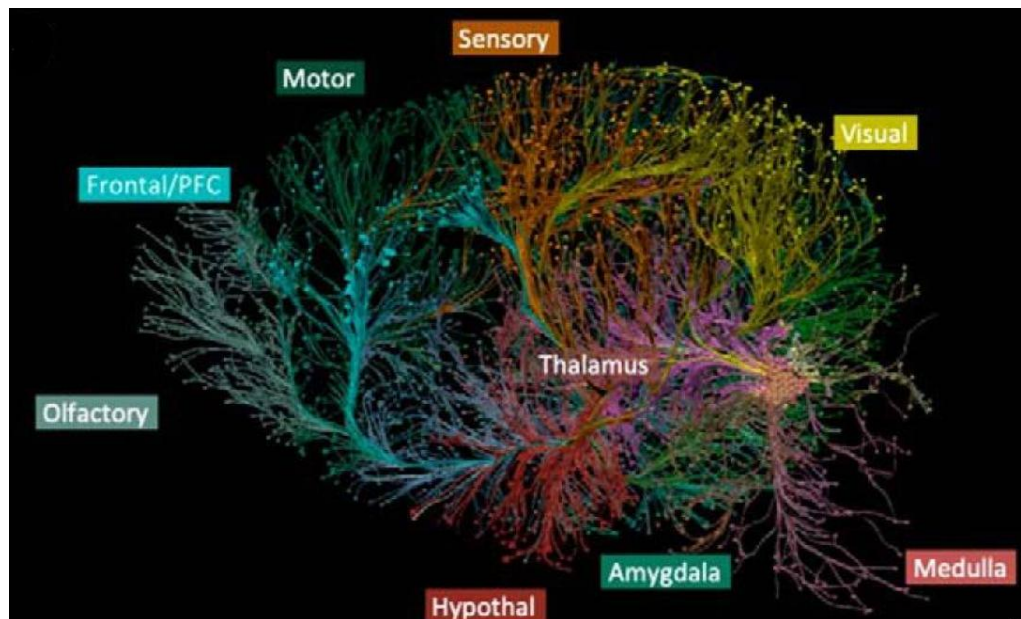
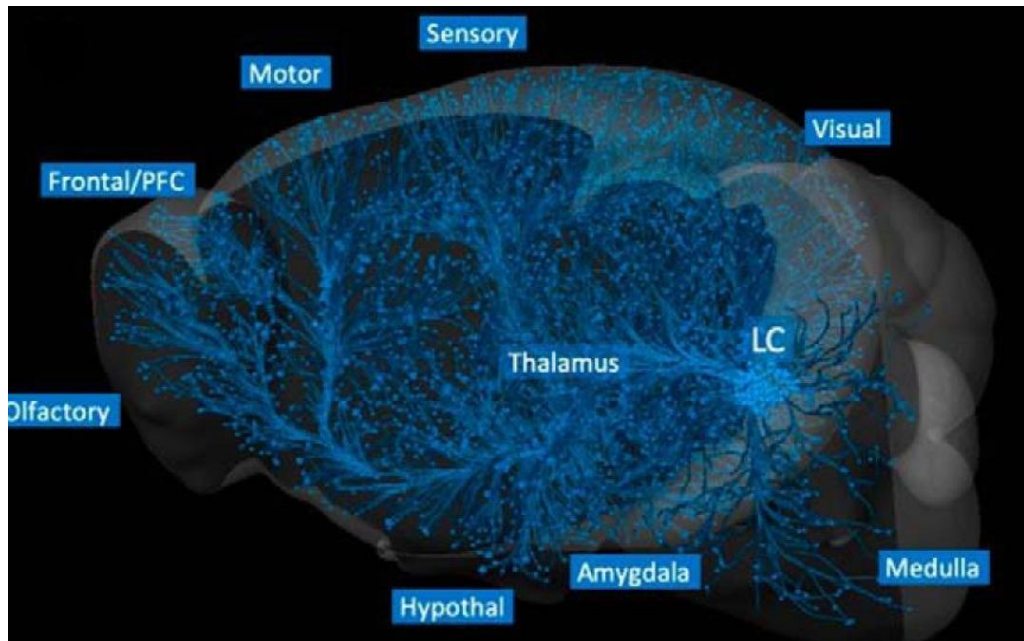


Figure 1. A reconstruction of LC projections reveals a modular organization. An enhanced green fluorescent protein (EGFP) tracing in a tyrosine hydroxylase-Cre mouse allows the visualization of the LC's widespread projection network ipsilateral to the injection, establishing a global fiber network across the brain (Top). The architecture with distinct fiber pathways reveals the suggested modular organization by mapping the projection axons to their target regions (Bottom). (Adapted from Chandler et al., 2019)

Recent research has revealed a complex range of behavioral and electrophysiological effects that suggest a common function for LC: enhancing the processing of relevant or salient information. This involves two main levels of action. First, the system plays a role in initiating and maintaining behavioral and neuronal states in the forebrain that are suited for gathering sensory information. Second, while awake, this system modulates the processing and collection of significant sensory input through a variety of concentration-dependent actions within cortical and subcortical circuits involved in sensory processing, attention, and memory (Berridge et al., 2003). The ability of a stimulus to increase discharge activity in the locus coeruleus seems to be unrelated to its valence. Taken together, these findings suggest that the locus coeruleus-noradrenergic system is an essential component of the neural networks that enable an animal to appropriately allocate attention to the most salient features of a complex environment (Sara 2009).

Norepinephrine

The LC noradrenergic nucleus was one of the first neuromodulator systems to be mapped anatomically and identified neurochemically, making it also one of the most extensively studied systems alongside dopamine and acetylcholine. The noradrenergic projection from the LC extends to nearly every brain region and serves as the primary source of norepinephrine everywhere in the forebrain (Sara 2009) with the exception of the striatum. Norepinephrine, a monoamine neurotransmitter, plays a crucial role in regulating cortical function. It is released by the ascending projections of the locus coeruleus (Berridge et al., 2003). Following an action potential, norepinephrine is

released into the synapse and binds to three main receptor subtypes: alpha-1, alpha-2, and beta receptors. These receptors are G-protein coupled and produce either inhibitory or excitatory effects, with varying binding affinities for norepinephrine (Gannon et al., 2015).

Alpha-1 receptors are G protein-coupled receptors associated with the heterotrimeric G protein, Gq/11 family, (Zhong et al, 1999) and are further divided into subtypes: alpha-1a, alpha-1b, and alpha-1d, and are located in post-synaptic areas to the locus coeruleus, the olfactory bulb, cerebral cortex, dentate gyrus, amygdala, and thalamus (Gannon et al., 2015). These receptors have an intermediate binding affinity for norepinephrine. Alpha-2 receptors are subdivided into alpha-2a, alpha-2b, and alpha-2c, and can be found in both presynaptic and postsynaptic areas of neurons in regions including the locus coeruleus, amygdala, and hypothalamus, with these receptors having the highest binding affinity for norepinephrine (Mandela et al., 2006). Beta receptors, including beta-1, beta-2, and beta-3 subtypes, are spread across various regions of the brain, with beta-1 and beta-2 receptors being most abundant in the cerebral cortex. These receptors exhibit the lowest binding affinity for norepinephrine (Mandela et al., 2006).

The most common method for clearing norepinephrine from the synaptic cleft is reuptake. The norepinephrine transporter (NET), located on presynaptic terminals, is one of the most common sodium-chloride-dependent transporter that mediates the reuptake of norepinephrine into the presynaptic terminal (Gannon et al., 2015). Once inside, it can either be degraded or stored in vesicles for future release (Mandela et al., 2006).

Lateral Habenula

Unexpected experiences can result in either positive or negative outcomes, and nearly all animal species are capable of quickly performing specific behaviors in response to these stimuli. This ability allows the brain to integrate external stimuli and generate responses based on previously unknown associations. Numerous brain structures are involved in the expression of both innate and learned behaviors, one of which is the habenula. The habenula is an epithalamic structure consisting of medial (MHb) and lateral (LHb) subregions. It receives a wide range of input from the basal ganglia, frontal cortex, basal forebrain, hypothalamus, and other areas involved in processing sensory information and internal states (Wallace et al., 2020). The LHb in particular has garnered considerable research interest due to its role in processing reward and aversive information, cognitive flexibility, and emotions (Hikosaka et al., 2008). It is an evolutionarily old and phylogenetically conserved nucleus in the brain. The LHb consists of several subnuclei, which form medial and lateral divisions (Wallace et al., 2020, Illustration 1). The medial division receives input primarily from limbic brain regions, which are directly or indirectly connected to the cerebral cortex, including basal forebrain structures such as the ventral pallidum, substantia innominata, and diagonal band, as well as parts of the extended amygdala, including the bed nucleus of the stria terminalis (Hikosaka et al., 2008). The lateral division, on the other hand, is innervated by the basal ganglia, particularly the internal segment of the globus pallidus, which receives cortical input through the striatum (Hisosaka et al., 2008). These parallel circuits allow extensive information processed by the cerebral cortex to converge at the LHb, which acts as a

crucial junction for limbic and basal ganglia pathways. The LHb also receives inputs from various forebrain limbic circuits that play a role in motivation and value processing and sends outputs to brainstem centers involved in predicting aversive events and regulating behavioral inhibition (Baker et al., 2016). It is activated by aversive stimuli and reward omission, while it is inhibited by unexpected rewards. As a result, the LHb is strategically positioned within the brain, with the necessary connectivity to both encode and predict valued external stimuli.

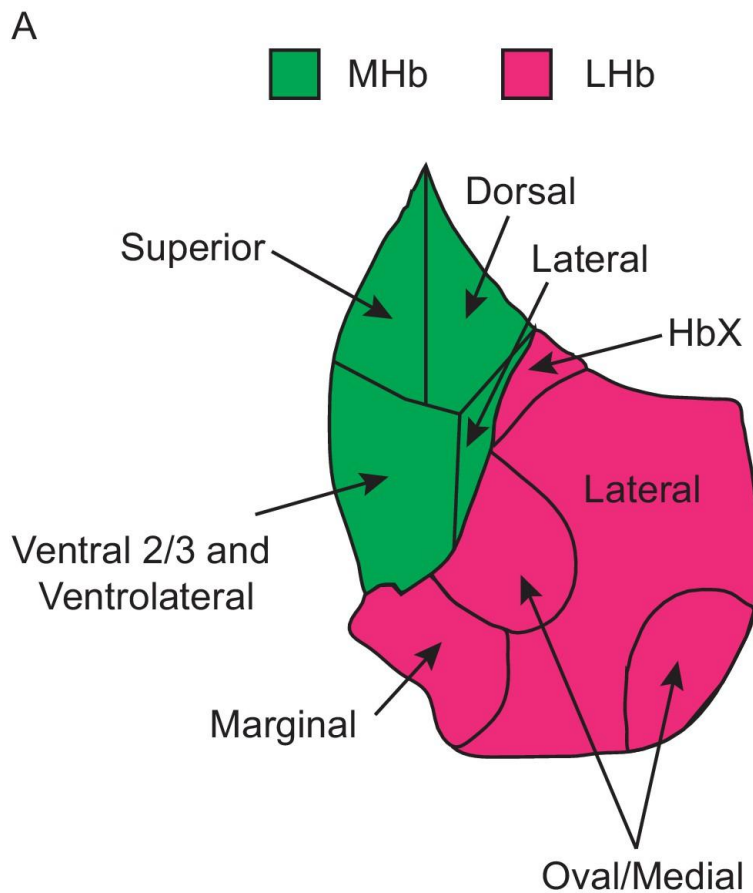


Illustration 1. A schematic illustrating a map of the subregions of the habenula based on single-cell transcriptomic profiling. The habenular subregions are outlined in black, with MHb subregions in green and LHb subregions in magenta. The border locations provide a rough

estimate of the boundary between transcriptionally defined neuronal subtypes, which have been confirmed through previous studies (Adapted from Wallace et al. 2020).

Reward Prediction

The LHb is able to exert top-down control over monoaminergic systems and respond to unexpected aversive stimuli. It has also been shown in previous research to be involved in responding to external cues that predict upcoming rewards or punishments (Mondolini et al. 2022). As a result, the LHb regulates both innate behaviors triggered by unpredicted stimuli and learned behaviors driven by predictive cues. LHb neurons are excited by reward omission or punishment and inhibited by unexpected rewards or their predictors (Wallace et al. 2020). Notably, this encoding mechanism is conserved across species, being present in humans, fish, and rodents alike (Mondolini et al. 2022). Given that the LHb plays a crucial role in processing positive and negative stimuli, it is expected that manipulating its function would influence behaviors related to the encoding of reward and aversion.

DSP-4

N-(2-chloroethyl)-N-ethyl-2-bromobenzylamine (DSP-4) is a monoaminergic neurotoxin that specifically targets and damages noradrenergic projections from the locus coeruleus, while also temporarily affecting peripheral sympathetic neurons (Bortel 2022). DSP-4 primarily functions by inhibiting norepinephrine reuptake, leading to increased NE release and a higher turnover rate of NE within the affected neurons, effectively depleting norepinephrine stores in the brain. DSP-4 can cross the blood-brain barrier, with its effects primarily limited to noradrenergic neurons in the CNS; but, it can also slightly reduce levels of dopamine and 5-hydroxytryptamine (Bortel 2022). When

administered systemically, DSP-4 rapidly and dose-dependently depletes endogenous norepinephrine levels by inhibiting its reuptake (Bromek 2022). The norepinephrine transporter on the neuronal plasma membrane is responsible for recapturing released norepinephrine into the presynaptic cell, maintaining neurotransmitter system balance. DSP-4 undergoes intramolecular cyclization to form an aziridinium ion, a highly reactive electrophilic intermediate that can hydrolyze or react with nucleophiles in biological tissues (Bortel 2022). This aziridinium ion, structurally similar to bretylium which is a substrate for NET, covalently and irreversibly binds to electrophilic centers near the NET's binding site. This disrupts its function and inhibits NE reuptake (Bortel 2022) leading to an eventual loss of NE within the brain.

Behavioral Task

To investigate probabilistic decision-making, mice were trained in a variation of the two-armed bandit (2ABT) behavioral task that allows for the manipulation and observation of LHb circuit dynamics *in vivo* during a thirst-motivated behavior. During each behavioral session, the water-restricted mouse was allowed to move freely within a chamber containing three ports, separated by physical barriers, into which it could place its snout to engage in the task (Illustration 1). A blue LED above the central port signaled that the mouse could initiate a trial by placing its snout or “poking” into the center port. The mouse then had to choose between poking into either the left or right port, each of which probabilistically delivered water after the snout entry. One of the side ports provided a reward with a higher probability (the highly rewarding port), while the other provided a reward with a lower probability. The mouse terminates the trial by

withdrawing from the side port, which initiates the intertrial interval state. This task was organized into blocks, where, after 50 rewards were obtained, the reward probabilities were reversed, known as a block transition. To maximize reward acquisition, the mouse learns to identify the highly rewarding port in each block and detect block transitions. This structure demands that the mouse employ flexible decision-making strategies, integrating information from previous trial outcomes to guide its choices.

The process of selecting an action, assessing it, and storing the outcome to guide future responses involves the basal ganglia and extended circuits like the LHb. Activity in the LHb is observed in various human neurological disorders where action selection is impaired. Additionally, the LHb likely functions as a key hub for the interaction between stress and decision-making. In the LHb, NE is known to play a role in both arousal and anxiety states. However, the precise mechanisms underlying LHb function and its interaction with NE during action evaluation are not yet fully understood. Gaining insight into LHb function in action selection is crucial for understanding how disruptions in these circuits contribute to dysfunction and disease.

Hypothesis

NE signaling is necessary for port switching and retention of the 2ABT task due to its role in attention allocation and working memory therefore, ablation of NE should result in decreased switching and performance.

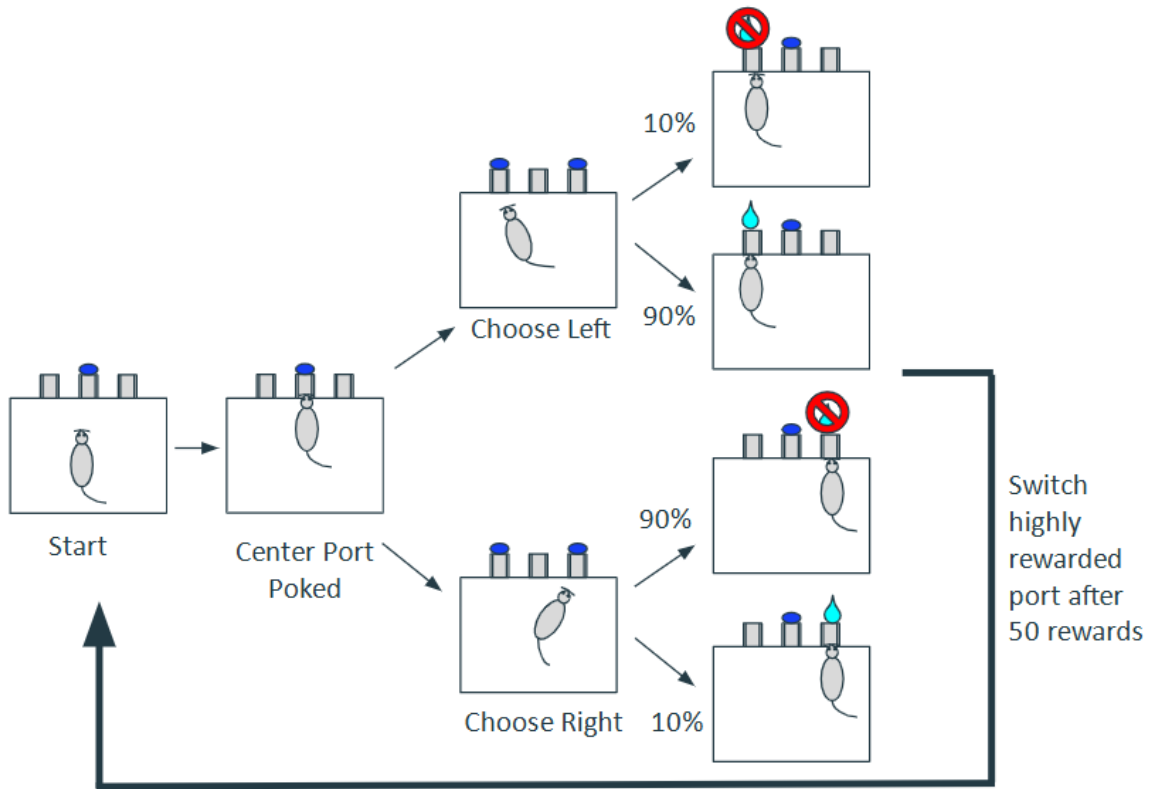


Illustration 2. A schematic illustrating the mouse movements in the probabilistic two-port choice task as well as the parameters. A blue LED in the center port signals a new trial can be initiated. A mouse initiates a trial by poking into the center port. It then selects one of the two side ports to enter the choice state. Depending on the choice and preassigned port reward probabilities, a single reward is or is not probabilistically delivered. After receiving 50 rewards regardless of the port chosen, the probabilities of the 2 ports are flipped.

MATERIALS AND METHODS

Experimental Subjects

The following mouse line was used: C57BL6/J (The Jackson Laboratory, 000664). The animals were maintained on a 12:12 reverse light/dark cycle in standard housing conditions with free access to food but restricted access to water. For behavioral experiments, both male and female mice, aged 8 weeks, were utilized. A minimum sample size of 16 was selected for all experiments, chosen independently of any statistical analysis. To reduce bias, the researcher was blinded to the treatment allocation of the mice. All procedures adhered to protocols approved by the Boston University Institutional Animal Care and Use Committee, in compliance with the U.S. National Institutes of Health Guide for the Care and Use of Laboratory Animals and American Association for Accreditation of Laboratory Animal Care (AAALAC) certified.

Injections

N-(2-Chloroethyl)-N-ethyl-2-bromobenzylamine (DSP-4) was obtained from Sigma (St. Louis, USA). According to existing literature, norepinephrine (NE) depletion is more significant following intravenous (i.v.) than intraperitoneal (i.p.) injection in adult rats (Bortel 2023) . However, i.p. administration is still effective in producing substantial NE depletion of up to 95% (Bortel 2023). A 50 mg/kg dose of DSP-4 is the most effective for inducing a marked and long-lasting reduction in NE reuptake in the central nervous system (CNS) without causing lethal effects in rats and mice (Bromek 2022). Solutions were prepared on the day of injection. DSP-4 was dissolved in isotonic saline and administered intraperitoneally at a dose of 50 mg/kg dissolved in enough saline to

reach a volume of 0.7 mL. Control mice were injected with 0.7 mL of saline. Mice received a total of three injections throughout the course of the experiment.

Mouse ID	Cage #	Genotype	Sex	Injection Date	Injection Type	Perfusion Date	IHC Date
170	C00122068	C57B16/j	M	1: 7/26/24 2: 8/02/24 3: 8/16/24	DSP4	8/26/24	12/17/24 - 12/18/24
171	C00122060	C57B16/j	M	1: 7/26/24 2: 8/02/24 3: 8/16/24	Saline	8/26/24	12/17/24 - 12/18/24
172	C00122065	C57B16/j	M	1: 7/26/24 2: 8/02/24 3: 8/16/24	DSP4	8/26/24	12/17/24 - 12/18/24
173	C00122062	C57B16/j	M	1: 7/26/24 2: 8/02/24 3: 8/16/24	Saline	8/26/24	12/17/24 - 12/18/24
174	C00122070	C57B16/j	F	1: 7/26/24 2: 8/02/24 3: 8/16/24	DSP4	8/26/24	12/18/24 - 12/19/24
175	C00122071	C57B16/j	F	1: 7/26/24 2: 8/02/24 3: 8/16/24	Saline	8/26/24	12/18/24 - 12/19/24
176	C00122074	C57B16/j	F	1: 7/26/24 2: 8/02/24 3: 8/16/24	DSP4	8/26/24	12/18/24 - 12/19/24
177	C00122064	C57B16/j	M	1: 7/26/24 2: 8/02/24 3: 8/16/24	DSP4	8/26/24	12/18/24 - 12/19/24
178	C00122063	C57B16/j	M	1: 7/26/24 2: 8/02/24 3: 8/16/24	Saline	8/26/24	12/19/24 - 12/20/24
179	C00122066	C57B16/j	M	1: 7/26/24 2: 8/02/24 3: 8/16/24	DSP4	8/27/24	12/19/24 - 12/20/24

180	C00122069	C57B16/j	M	1: 7/26/24 2: 8/02/24 3: 8/16/24	Saline	8/27/24	12/19/24 - 12/20/24
181	C00124651	C57B16/j	F	1: 7/26/24 2: 8/02/24 3: 8/16/24	Saline	8/27/24	12/19/24 - 12/20/24
182	C00124655	C57B16/j	F	1: 7/26/24 2: 8/02/24 3: 8/16/24	DSP4	8/27/24	12/24/24 - 12/25/24
183	C00122059	C57B16/j	F	1: 7/26/24 2: 8/02/24 3: 8/16/24	Saline	8/27/24	12/24/24 - 12/25/24
184	C00122061	C57B16/j	F	1: 7/26/24 2: 8/02/24 3: 8/16/24	DSP4	8/27/24	12/24/24 - 12/25/24
185	C00124650	C57B16/j	F	1: 7/26/24 2: 8/02/24 3: 8/16/24	Saline	8/27/24	12/24/24 - 12/25/24

Table 1. A table listing the experimental subjects, their sex, treatment type, date of treatment, perfusion, and IHC.

Behavior Apparatus and Training

The apparatus used for the behavior is as described previously (Chantranupong et al., 2023; Beron et al., 2022; Locantore et al., 2025) with the following modifications.

Clear acrylic barriers 5.5 cm in length were installed in between the center and side ports to extend the trial time to aid in better behavior recordings. Water was delivered in 3 μ L increments. Hardware and software to control the behavior box are available online at <https://github.com/HMS-RIC/TwoArmedBandit>.

Mice were water-restricted prior to training, maintained at 80-85% of their initial body weight, and housed individually throughout the entire training and experimental period. All training sessions were carried out in the dark under red-light conditions.

During the task, a blue LED above the center port signaled the mouse to begin a trial by poking into the center port. Once the mouse did so, blue LEDs above the side ports were activated, prompting the mouse to choose and poke into either the left or right side port within 2 seconds. The reward probabilities for the side ports were controlled by custom software (MATLAB) and ranged from 10-90%, depending on the specific experiment. Withdrawal from the side port ended the trial and triggered a 1-second intertrial interval (ITI). A well-trained mouse could complete 300-600 trials within a 40-minute session.

To train the mice to proficiency, they underwent a series of incremental training phases (Illustration 2). Each session lasted 40 minutes and was adapted based on the mouse's performance. On the first day, phase 0, the mice were weighed and water-restricted for 2 days in order to drop to 80-85% body weight. On day 3 mice began phase 1 in which case they were habituated to the behavior box, with water being delivered from both side ports and triggered only by a side port poke. After receiving 150+ rewards for 2 days in a row, mice were moved onto the next phase. In phase 1b, mice learned the trial structure in which case only a poke in the center port followed by a side port poke would deliver water. Mice had a 15-second (s) window after the center poke to choose a side port before the trial would automatically end. After 2 days with 100+ rewards, mice moved onto phase 2 where the window between center port poke and side port poke would incrementally be dropped to 2 seconds. Also in phase 2, the mice were trained to learn the block structure, in which 50 rewarded trials on one side port trigger the reward probabilities to switch. The probabilities in this phase were 100% and 0% so the highly rewarded port delivered water 100% of the time while the other port delivered no reward.

After 100+ rewards with the 2 s window, mice were moved onto the final stage of training. Phase 3 was introducing the 2ABT with 90-10 reward probabilities. Mice remained in this training phase until they met the well-trained criteria in which they would choose the highly rewarding port 75% of the time for at least 3 days in a row. Once all mice achieved this criterion, they were moved on to begin the experiment.

At the start of the experiment, mice were run on the 2ABT at 90-10 probabilities for 6 days to achieve a baseline. The mice then received the first injection of either DSP-4 or saline on Friday and were allowed the weekend to recover. Experimental data was collected for 4 days and experimental mice received their second injection of DSP-4 while control mice received their second dose of saline and allowed the weekend to recover. Experimental data was collected for 10 days and the mice received their 3rd and final respective injections and allowed the weekend to recover. The mice were run on 70-30 probabilities for 5 days and perfused at the start of the following week.

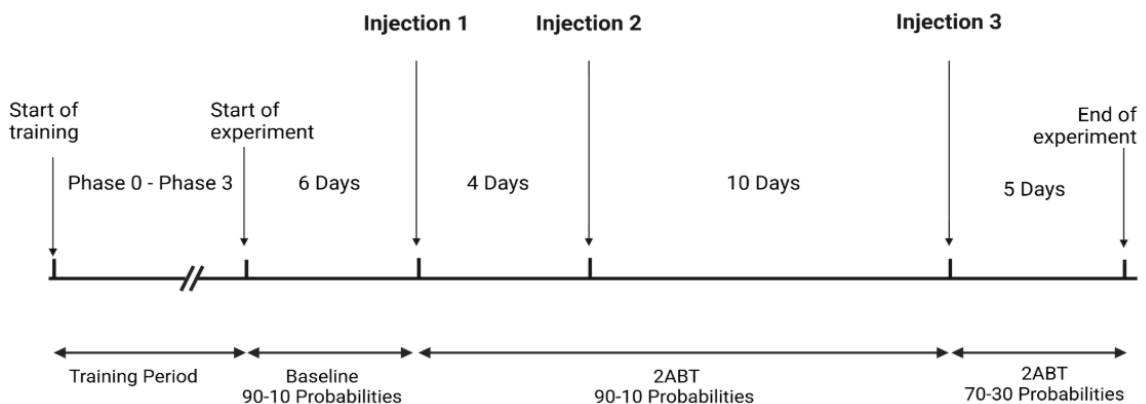


Illustration 3. A schematic illustrating the experimental timeline. Mice started training at phase 0 and progressed through phases 1, 1b, 2, and 3. After meeting the criteria for well-trained ($P(\text{Select highly rewarded port}) > 0.75$ for 5 days in a row), mice were run for 6 days to measure baseline. Afterward, the mice received the injection with a weekend to recover and were run on

the behavioral task the following week(s). The mice were run on 90-10 probabilities for the first 2 injections and 70-30 probabilities after the 3rd injection.

Immunohistochemistry Protocol

Mice were deeply anesthetized with isoflurane and underwent transcardiac perfusions with 4% paraformaldehyde (PFA) in 0.1 M sodium phosphate buffer saline (PBS). Brains were post-fixed overnight in 4% PFA and 0.02% sodium azide in PBS. The next day the brains were immersed in 30% (wt/vol) sucrose with 0.02% sodium azide in PBS for long-term storage at 4 °C. The brains were sectioned coronally at 50 µm using a Freezing Microtome (Leica). Selected brain slices were placed in a six-well plate and rinsed three times for 5 minutes each in PBS. The free-floating sections were permeabilized and blocked with 5% normal goat serum in PBS containing 0.2% Triton X-100 (blocking buffer) for 1 hour at room temperature and then incubated with primary antibodies at 4 °C overnight with side-to-side rotation. The following day, slices were transferred to a clean well and washed five times for 5 minutes each in wash buffer (blocking buffer diluted 1:10 with PBS). They were then incubated with secondary antibodies for 1 hour at room temperature in wash buffer. Afterward, slices were washed in wash buffer for 5 minutes then in wash buffer supplemented with one drop of NucBlue for 7 minutes, both at room temperature. The sections were subsequently washed four times in PBST and four times in PBS, each for 5 minutes. Brain sections were mounted on Superfrost slides, allowed to dry, and a cover slip was placed on with ProLong Diamond Antifade Mountant. Primary antibodies used were Mouse anti-NET (1:800, NET05-2 MAb) and Rabbit anti-TH (1:800, AB152, Abcam). Alexa Fluor 647- and 750-

conjugated secondary antibodies to mouse and rabbit (Invitrogen) were diluted 1:500.

Whole sections were imaged using an Olympus VS200 slide scanning microscope. All images underwent identical manipulations for quantitative comparison.

RESULTS

90-10

In order to examine the effects of NE on motivated behavior a dynamic, probabilistic switching task was employed in mice modeled after behavioral paradigms shown to require basal ganglia circuitry (Chantranupong et al., 2023; Wallace et al., 2025). The mice were water-restricted and placed in a behavioral box with three nose-poke ports separated by dividers. The water rewards were delivered asymmetrically at 90-10 probabilities in a block structure such that once 50 rewards were gained, the reward probabilities were flipped between the ports. A well-trained animal uses its history of choices (left or right) and outcomes (rewarded or unrewarded) to inform future actions and is sensitive to these block transitions (Supp. Fig. 1).

The weight of the animals was measured every day the task was run and the data was calculated as the percent of each animal's original (pre-water restriction) body weight. This data was compared across both DSP-4 and Saline injected mice during the baseline, first, and second injection conditions using a nested ANOVA (Figure 2). Comparisons made between Saline Baseline – DSP4 Baseline, Saline Baseline – Saline Injection 1, DSP4 Baseline – DSP4 Injection 1, Saline Injection 1 – DSP4 Injection 1, and Saline Injection 2 – DSP4 Injection 2 resulted in no statistically significant differences. However, comparisons between Saline Baseline – Saline Injection 2 and DSP4 Baseline – DSP4 Injection 2 showed statistical significance. The mice appear to have gained weight, getting closer to their original body weight. There was also significant variance among the mice in each injection group.

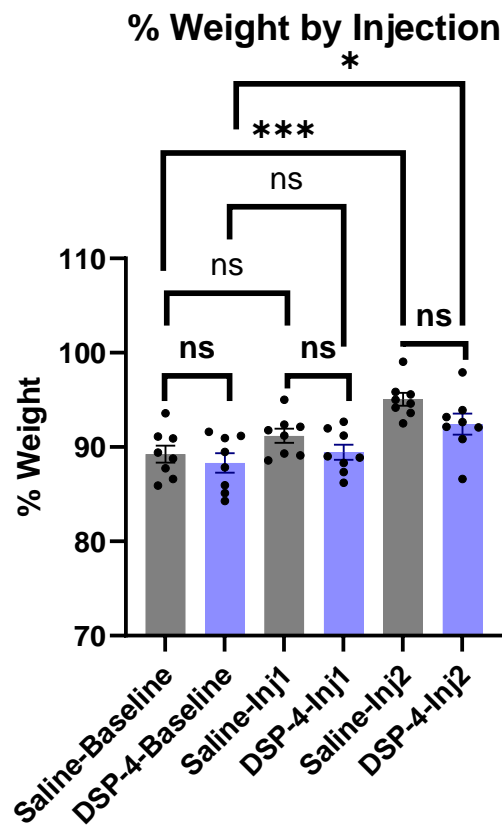


Figure 2. The average percent body weight of DSP-4 and Saline injected mice during 90-10 reward probabilities compared across the baseline, first and second injections (bar = mean, error bar = SEM) (nested ANOVA $F = 7.960$, $DFn = 5$, $DFd = 42$, p -values: <0.0001).

The probability of the mice choosing the highly rewarded port was calculated during each session. This data was compared across both DSP-4 and Saline injected mice during the baseline, first, and second injection conditions using a nested ANOVA (Figure 3). Comparisons were made between Saline Baseline – DSP4 Baseline, Saline Baseline – Saline Injection 1, DSP4 Baseline – DSP4 Injection 1, Saline Baseline – Saline Injection 2, DSP4 Baseline – DSP4 Injection 2, Saline Injection 1 – DSP4 Injection 1, and Saline Injection 2 – DSP4 Injection 2 and each showed no statistical significance. The well-trained mice on average appear to have no trouble choosing the

highly rewarded port each session. However, there was some significant variance among the mice in each injection group.

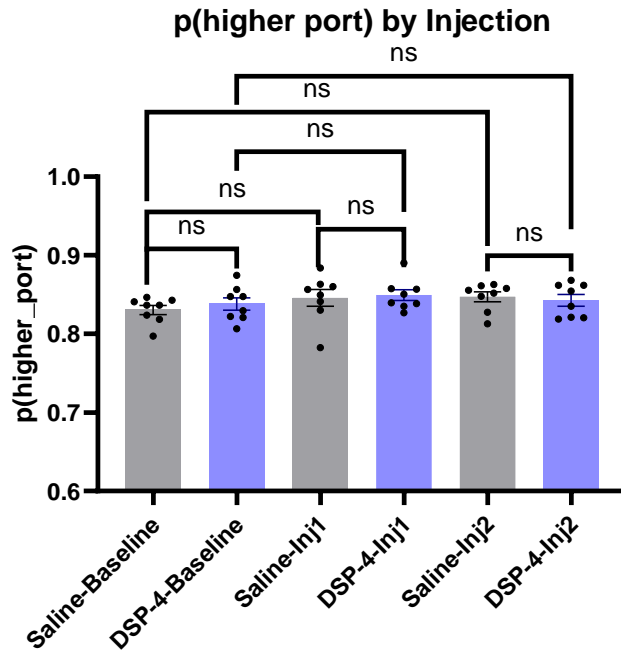


Figure 3. The probability of DSP-4 and Saline injected mice choosing the highly rewarded port on all trials during 90-10 reward probabilities across the baseline, first and second injections (bar = mean, error bar = SEM) (nested ANOVA $F = 7.818$, $DFn = 5$, $DFd = 42$, p -values: 0.5685)

The probability of the mice receiving a reward was calculated during each session as well and appears to follow a similar trend as the probability of choosing the highly rewarded port. This data was compared across both DSP-4 and Saline injected mice during the baseline, first, and second injection conditions using a nested anova (Figure 4). Comparisons were made between Saline Baseline – DSP4 Baseline, Saline Baseline – Saline Injection 1, DSP4 Baseline – DSP4 Injection 1, Saline Baseline – Saline Injection 2, DSP4 Baseline – DSP4 Injection 2, Saline Injection 1 – DSP4 Injection 1, and Saline Injection 2 – DSP4 Injection 2 and each showed no statistical significance. The well-trained mice on average appear to have no trouble choosing the highly rewarded port and

receiving a reward each session. However, there appears to be some significant variance among the mice within the injection groups.

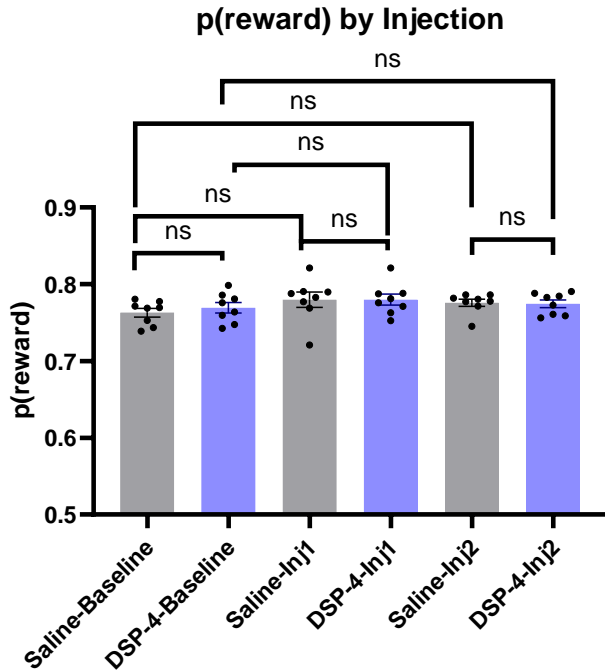


Figure 4. The probability of DSP-4 and Saline injected mice receiving a reward on all trials during 90-10 reward probabilities across the baseline, first and second injections (bar = mean, error bar = SEM) (nested ANOVA $F = 0.9974$, $DFn = 5$, $DFd = 42$, p -values: 0.4311)

The probability of switching during the task was calculated during each session but it was averaged across all trials. This data was compared across both DSP-4 and Saline injected mice during the baseline, first, and second injection conditions using a nested anova (Figure 5). Comparisons were made between Saline Baseline – DSP4 Baseline, Saline Baseline – Saline Injection 1, DSP4 Baseline – DSP4 Injection 1, Saline Baseline – Saline Injection 2, DSP4 Baseline – DSP4 Injection 2, Saline Injection 1 – DSP4 Injection 1, and Saline Injection 2 – DSP4 Injection 2 and each showed no statistical significance. The well-trained mice appear to switch less over time but this

difference is not significant. However, there was some very significant variance among the mice within the injection groups.

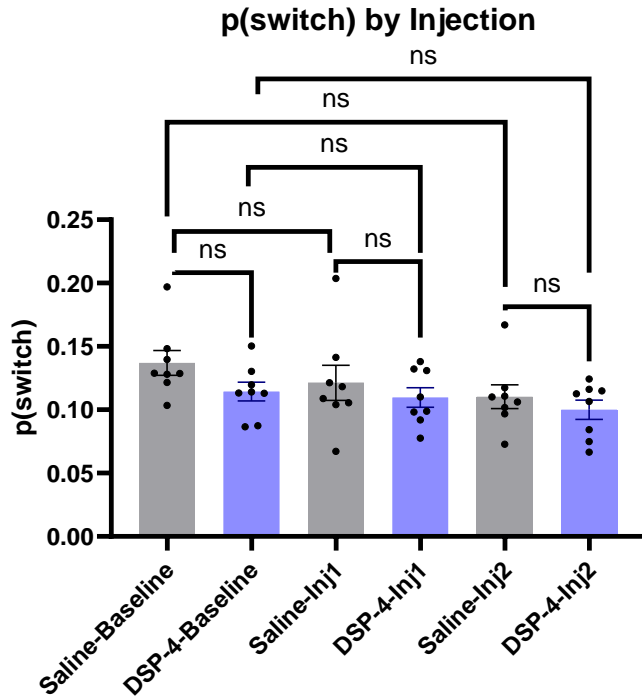


Figure 5. The probability of DSP-4 and Saline injected mice switching on all trials during 90-10 reward probabilities across the baseline, first and second injections (bar = mean, error bar = SEM) (nested ANOVA $F = 1.806$, $DFn = 5$, $DFd = 42$, p -values: 0.1325)

The total number of trials completed by each mouse during the task was calculated for each session. This data was compared across both DSP-4 and Saline injected mice during the baseline, first, and second injection conditions using a nested anova (Figure 6). Comparisons were made between Saline Baseline – DSP4 Baseline, Saline Baseline – Saline Injection 1, DSP4 Baseline – DSP4 Injection 1, Saline Baseline – Saline Injection 2, DSP4 Baseline – DSP4 Injection 2, Saline Injection 1 – DSP4 Injection 1, and Saline Injection 2 – DSP4 Injection 2 and each showed no statistical

significance. The well-trained mice appear to complete ~400 trials regardless of the injection group. However, there was some very significant variance among the mice within the injection groups.

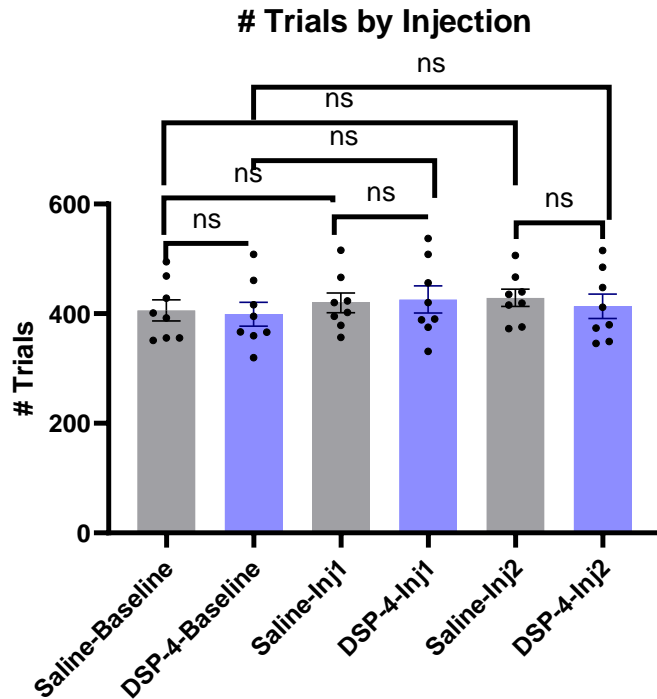


Figure 6. The average number of trials of DSP-4 and Saline injected mice performed during 90-10 reward probabilities across the baseline, first and second injections (bar = mean, error bar = SEM) (nested ANOVA $F = 0.3215$, $DFn = 5$, $DFd = 42$, p -values: 0.8973)

The intertrial interval during each trial was calculated and averaged across each session for each mouse. This data was compared across both DSP-4 and Saline injected mice during the baseline, first, and second injection conditions using a nested anova (Figure 7). Comparisons were made between Saline Baseline – DSP4 Baseline, Saline Baseline – Saline Injection 1, DSP4 Baseline – DSP4 Injection 1, Saline Baseline – Saline Injection 2, DSP4 Baseline – DSP4 Injection 2, Saline Injection 1 – DSP4

Injection 1, and Saline Injection 2 – DSP4 Injection 2 and each showed no statistical significance. However, there appears to be some very significant variance among the mice within the injection groups.

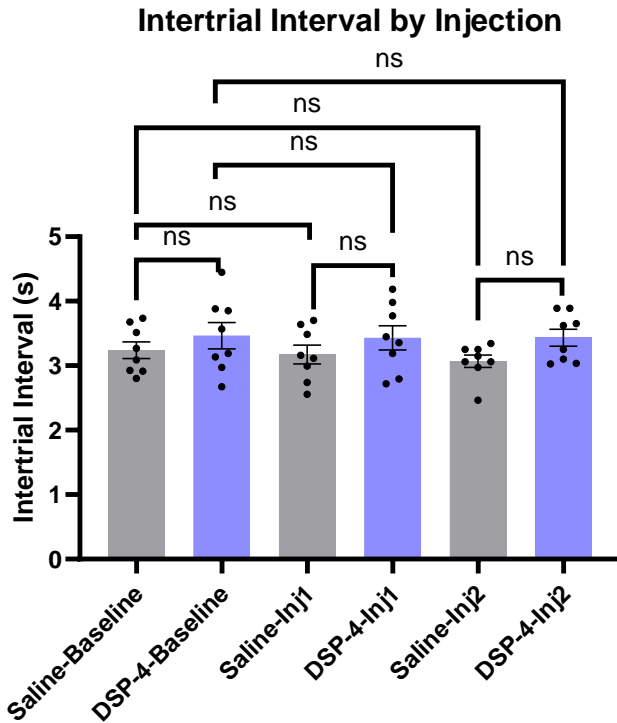


Figure 7. The average intertrial interval of DSP-4 and Saline injected mice during 90-10 reward probabilities across the baseline, first and second injections (bar = mean, error bar = SEM) (nested ANOVA $F = 1.190$, $DFn = 5$, $DFd = 42$, p -values: 0.3303)

The duration of each trial was calculated and averaged across the session for each mouse. This data was compared across both DSP-4 and Saline injected mice during the baseline, first, and second injection conditions using a nested anova (Figure 8).

Comparisons were made between Saline Baseline – DSP4 Baseline, Saline Baseline – Saline Injection 1, DSP4 Baseline – DSP4 Injection 1, Saline Baseline – Saline Injection 2, DSP4 Baseline – DSP4 Injection 2, Saline Injection 1 – DSP4 Injection 1, and Saline

Injection 2 – DSP4 Injection 2 and each showed no statistical significance. Well trained mice appear to take a little under 6 seconds to complete a trial regardless of injection group. However, there appears to be large amounts of variance among the mice within the injection groups.

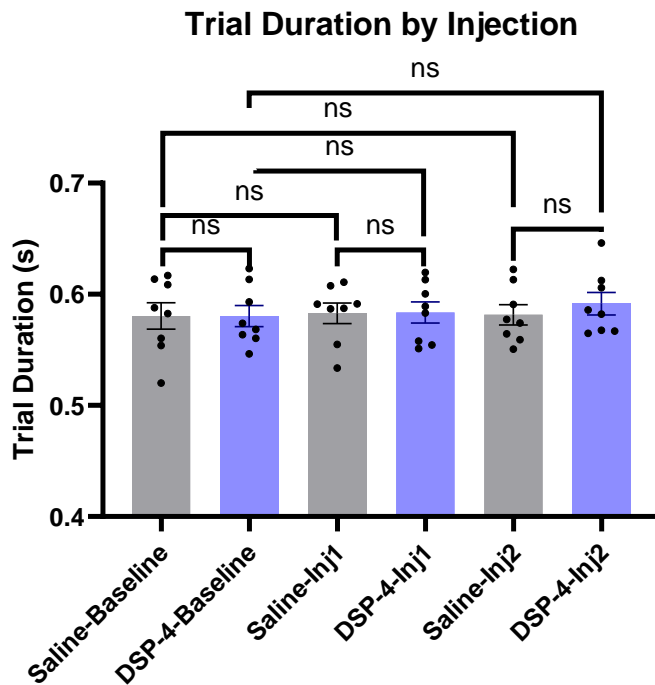


Figure 8. The average trial duration of DSP-4 and Saline injected mice during 90-10 reward probabilities across the baseline, first and second injections (bar = mean, error bar = SEM) (nested ANOVA $F = 0.1827$, $DFn = 5$, $DFd = 42$, p -values: 0.9676)

The probability of the mice choosing the left port was calculated across each session for every mouse. This data was compared across both DSP-4 and Saline injected mice during the baseline, first, and second injection conditions using a nested anova (Figure 9). Comparisons were made between Saline Baseline – DSP4 Baseline, Saline Baseline – Saline Injection 1, DSP4 Baseline – DSP4 Injection 1, Saline Baseline – Saline Injection 2, DSP4 Baseline – DSP4 Injection 2, Saline Injection 1 – DSP4

Injection 1, and Saline Injection 2 – DSP4 Injection 2 and each showed no statistical significance. It appears the mice had no preference for which port they would choose and chose the left port ~50% of the time regardless of the injection group.

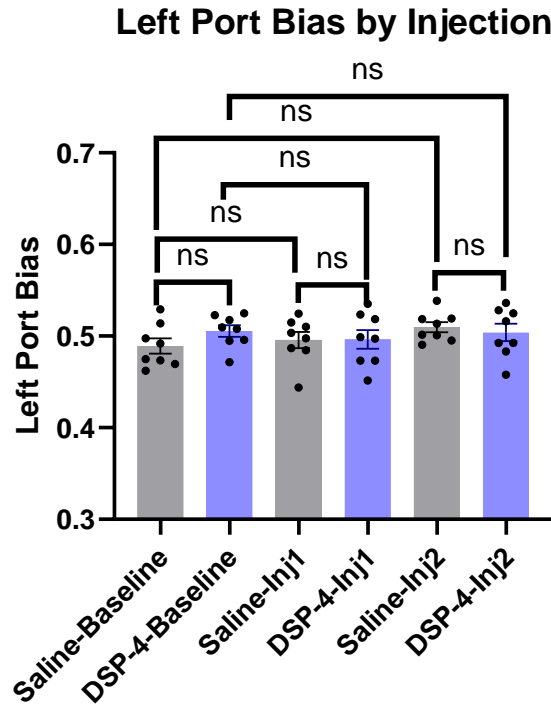


Figure 9. The probability of choosing the left port of DSP-4 and Saline injected mice during 90-10 reward probabilities across the baseline, first and second injections (bar = mean, error bar = SEM) (nested ANOVA $F = 0.9150$, $DFn = 5$, $DFd = 42$, p -values: 0.4807)

Male vs Female 90-10

Due to the variance seen within the groups, the data was further divided between male and female mice. The weight of the male mice was compared across both DSP-4 and Saline injected mice during the baseline, first, and second injection conditions using a nested anova (Figure 10). Then, the weight of the female mice was compared across both DSP-4 and Saline injected mice during the baseline, first, and second injection

conditions using a nested anova (Figure 10). In the male mice, comparisons made between Saline Baseline – Saline Injection 2 and DSP4 Baseline – DSP4 Injection 2 groups were statistically significant. However, in the female mice, only comparisons made between Saline Baseline – Saline Injection 2 showed any statistical significance. These mice appear to have gained weight, getting closer to their original body weight.

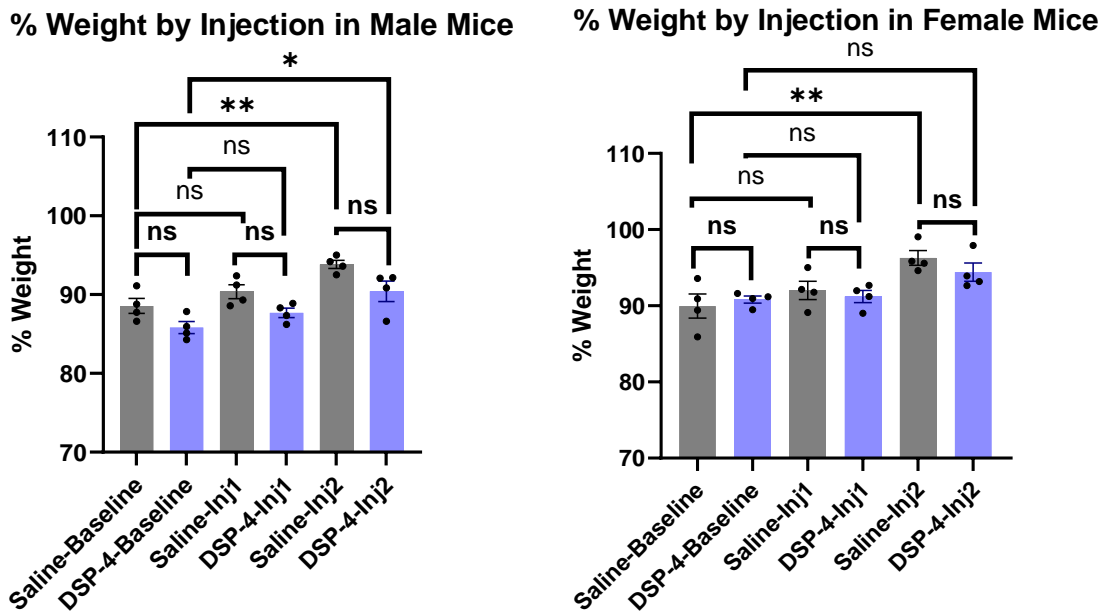


Figure 10. The average percent body weight of DSP-4 and Saline injected male mice (left) during 90-10 reward probabilities compared across the baseline, first and second injections (bar = mean, error bar = SEM) (nested ANOVA $F = 9.767$, $DFn = 5$, $DFd = 18$, p -values: 0.0001). The average percent body weight of DSP-4 and Saline injected female mice (right) during 90-10 reward probabilities compared across the baseline, first and second injections (bar = mean, error bar = SEM) (nested ANOVA $F = 5.113$, $DFn = 5$, $DFd = 18$, p -values: 0.0043).

The data showing the probability of choosing the highly rewarded port was also broken down between male and female mice. The male mice were compared across both DSP-4 and Saline injected mice during the baseline, first, and second injection conditions using a nested anova (Figure 11). Then, the female mice were compared across both

DSP-4 and Saline injected mice during the baseline, first, and second injection conditions using a nested anova (Figure 11). In the male mice, none of the comparisons made between groups were statistically significant. The same is true for the female mice, none of the comparisons showed any statistical significance.

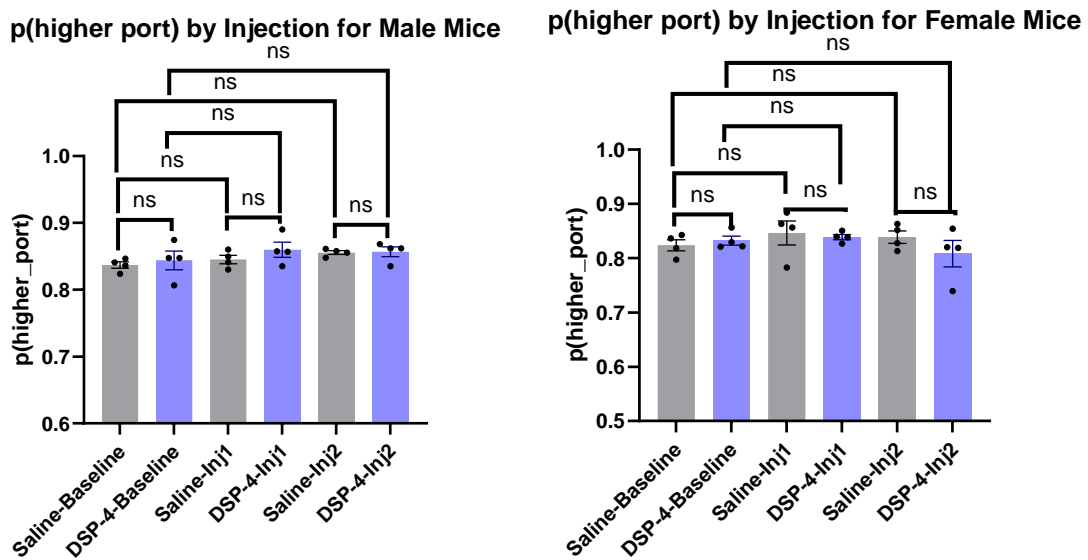


Figure 11. The probability of choosing the highly rewarding port for DSP-4 and Saline injected male mice (left) during 90-10 reward probabilities compared across the baseline, first and second injections (bar = mean, error bar = SEM) (nested ANOVA $F = 1.143$, $DFn = 5$, $DFd = 18$, p -values: 0.3743). The probability of choosing the highly rewarding port for DSP-4 and Saline injected female mice (right) during 90-10 reward probabilities compared across the baseline, first and second injections (bar = mean, error bar = SEM) (nested ANOVA $F = 0.6911$, $DFn = 5$, $DFd = 18$, p -values: 0.6367).

The data showing the probability of receiving a reward was also broken down between male and female mice and followed the same trend as the probability of choosing the highly rewarded port. The male mice were compared across both DSP-4 and Saline injected mice during the baseline, first, and second injection conditions using a nested anova (Figure 12). Then, the female mice were compared across both DSP-4 and Saline injected mice during the baseline, first, and second injection conditions using a

nested anova (Figure 12). In the male mice, none of the comparisons made between groups were statistically significant. The same is true for the female mice, none of the comparisons showed any statistical significance.

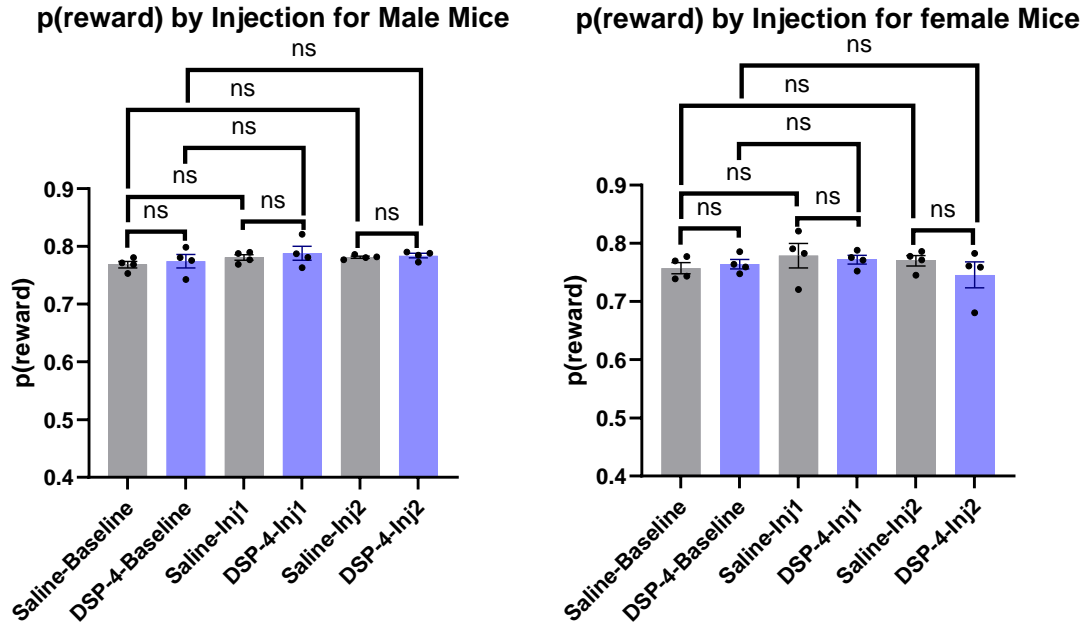


Figure 12. The probability of receiving a reward for DSP-4 and Saline injected male mice (left) during 90-10 reward probabilities compared across the baseline, first and second injections (bar = mean, error bar = SEM) (nested ANOVA $F = 0.9641$, $DFn = 5$, $DFd = 18$, p -values: 0.4654). The probability of receiving a reward for DSP-4 and Saline injected female mice (right) during 90-10 reward probabilities compared across the baseline, first and second injections (bar = mean, error bar = SEM) (nested ANOVA $F = 0.5871$, $DFn = 5$, $DFd = 18$, p -values: 0.7098).

The data showing the probability of switching was also broken down between male and female mice. The male mice were compared across both DSP-4 and Saline injected mice during the baseline, first, and second injection conditions using a nested anova (Figure 13). Then, the female mice were compared across both DSP-4 and Saline injected mice during the baseline, first, and second injection conditions using a nested anova (Figure 13). In the male mice, none of the comparisons made between groups were

statistically significant. The same is true for the female mice, none of the comparisons showed any statistical significance. Although it appears to decrease with each group, the data is not statistically significant.

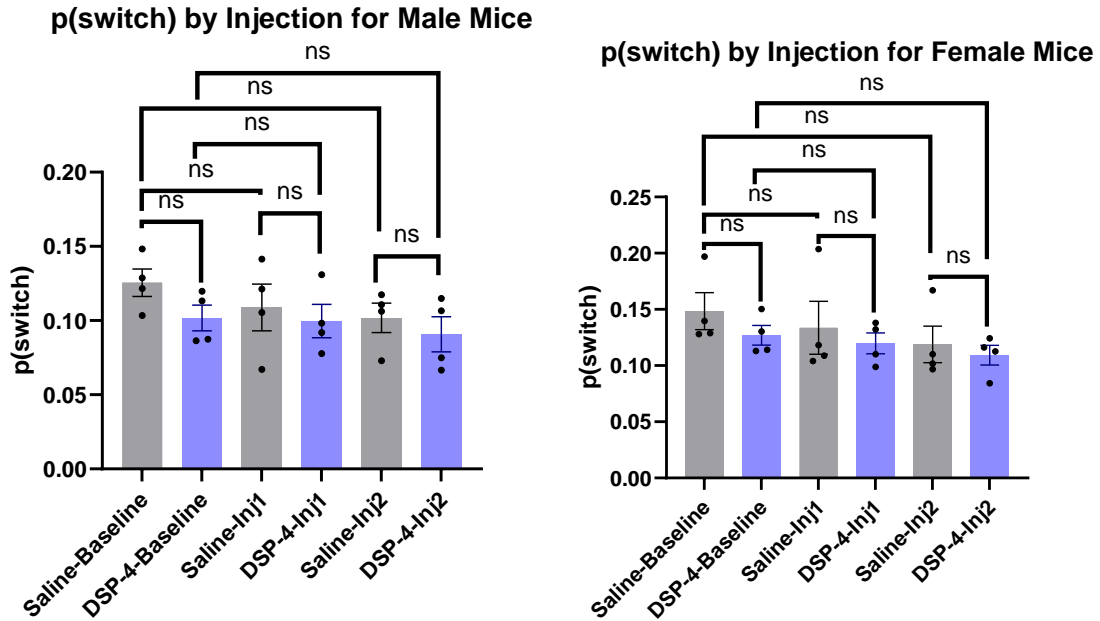


Figure 13. The probability of switching for all trials in DSP-4 and Saline injected male mice (left) during 90-10 reward probabilities compared across the baseline, first and second injections (bar = mean, error bar = SEM) (nested ANOVA $F = 1.109$, $DFn = 5$, $DFd = 18$, p -values: 0.3904). The probability of switching for all trials in DSP-4 and Saline injected female mice (right) during 90-10 reward probabilities compared across the baseline, first and second injections (bar = mean, error bar = SEM) (nested ANOVA $F = 0.8855$, $DFn = 5$, $DFd = 18$, p -values: 0.5109).

The data showing the average number of trials per session was also broken down between male and female mice. The male mice were compared across both DSP-4 and Saline injected mice during the baseline, first, and second injection conditions using a nested anova (Figure 14). Then, the female mice were compared across both DSP-4 and Saline injected mice during the baseline, first, and second injection conditions using a nested anova (Figure 14). In the male mice, none of the comparisons made between

groups were statistically significant. The same is true for the female mice, none of the comparisons showed any statistical significance.

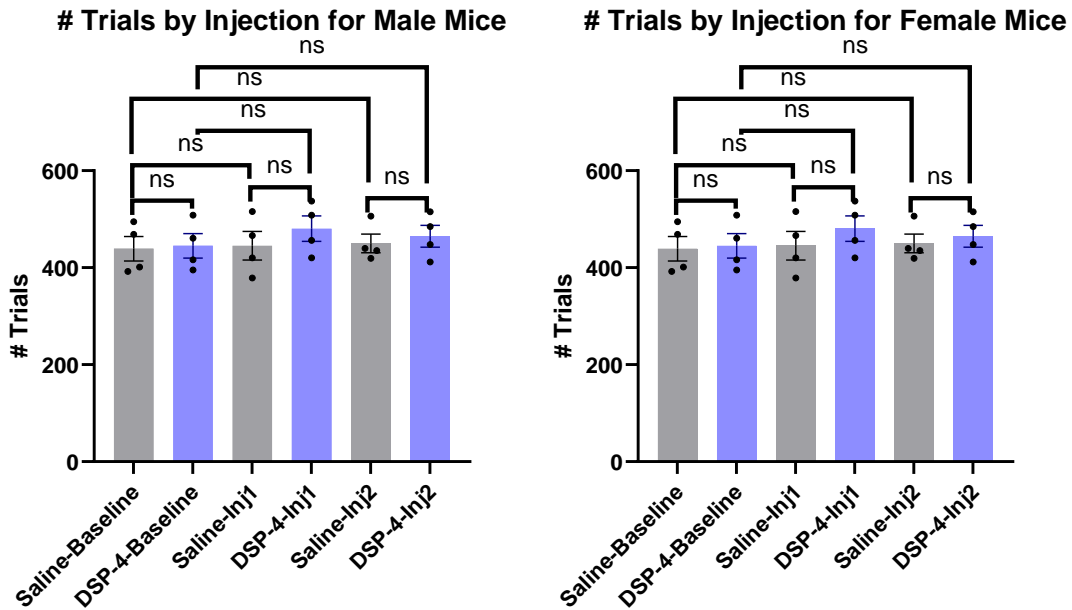


Figure 14. The average number of trials in DSP-4 and Saline injected male mice (left) during 90-10 reward probabilities compared across the baseline, first and second injections (bar = mean, error bar = SEM) (nested ANOVA $F = 0.3897$, $DFn = 5$, $DFd = 18$, p -values: 0.8494). The average number of trials in DSP-4 and Saline injected female mice (right) during 90-10 reward probabilities compared across the baseline, first and second injections (bar = mean, error bar = SEM) (nested ANOVA $F = 1.792$, $DFn = 5$, $DFd = 18$, p -values: 0.1653).

The data showing the intertrial interval averaged across each session for every mouse was also broken down between male and female mice. The male mice were compared across both DSP-4 and Saline injected mice during the baseline, first, and second injection conditions using a nested anova (Figure 15). Then, the female mice were compared across both DSP-4 and Saline injected mice during the baseline, first, and second injection conditions using a nested anova (Figure 15). In the male mice, none of

the comparisons made between groups were statistically significant. The same is true for the female mice, none of the comparisons showed any statistical significance.

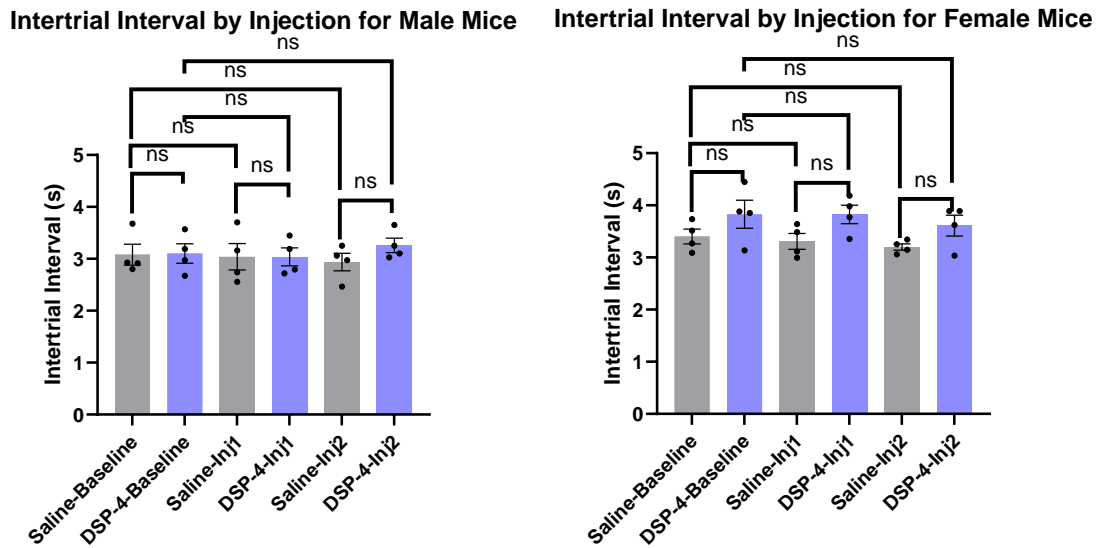


Figure 15. The average intertrial interval across all trials in DSP-4 and Saline injected male mice (left) during 90-10 reward probabilities compared across the baseline, first and second injections (bar = mean, error bar = SEM) (nested ANOVA $F = 0.2965$, $DFn = 5$, $DFd = 18$, p-values: 0.9085). The average intertrial interval across all trials in DSP-4 and Saline injected female mice (right) during 90-10 reward probabilities compared across the baseline, first and second injections (bar = mean, error bar = SEM) (nested ANOVA $F = 2.236$, $DFn = 5$, $DFd = 18$, p-values: 0.0952).

The data showing the average trial duration for each session was broken down between male and female mice. The male mice were compared across both DSP-4 and Saline injected mice during the baseline, first, and second injection conditions using a nested anova (Figure 16). Then, the female mice were compared across both DSP-4 and Saline injected mice during the baseline, first, and second injection conditions using a nested anova (Figure 16). In the male mice, none of the comparisons made between

groups were statistically significant. The same is true for the female mice, none of the comparisons showed any statistical significance.

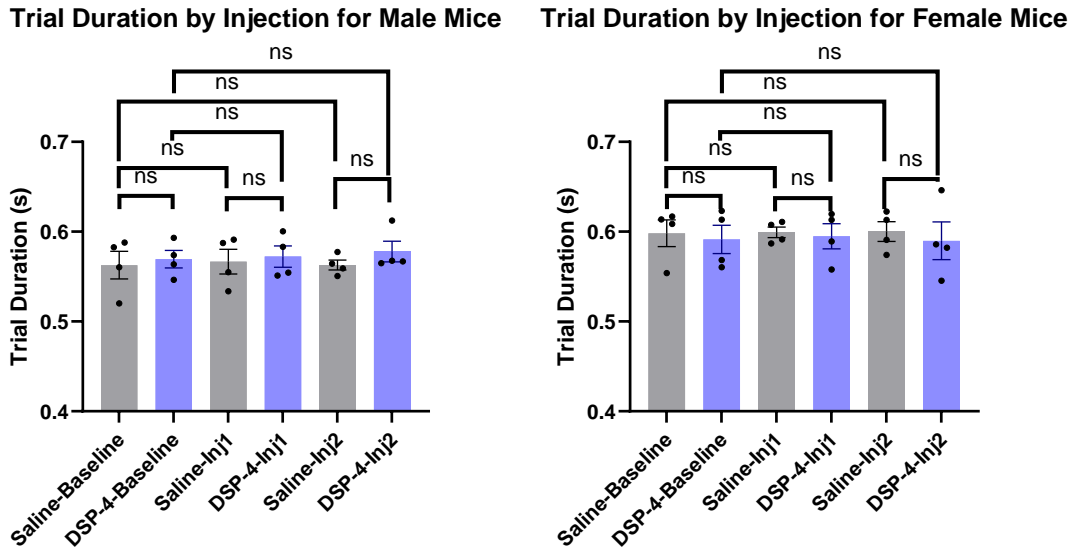


Figure 16. The average trial duration for all trials in DSP-4 and Saline injected male mice (left) during 90-10 reward probabilities compared across the baseline, first and second injections (bar = mean, error bar = SEM) (nested ANOVA $F = 0.2616$, $DFn = 5$, $DFd = 18$, p -values: 0.9282). The average trial duration for all trials in DSP-4 and Saline injected female mice (right) during 90-10 reward probabilities compared across the baseline, first and second injections (bar = mean, error bar = SEM) (nested ANOVA $F = 0.1277$, $DFn = 5$, $DFd = 18$, p -values: 0.9842).

The data showing the probability of choosing the left port was also broken down between male and female mic. The male mice were compared across both DSP-4 and Saline injected mice during the baseline, first, and second injection conditions using a nested anova (Figure 17). Then, the female mice were compared across both DSP-4 and Saline injected mice during the baseline, first, and second injection conditions using a nested anova (Figure 17). In the male mice, none of the comparisons made between groups were statistically significant. The same is true for the female mice, none of the

comparisons showed any statistical significance. It appears the mice did not have a preference for either port, choosing the left port ~50% of the time.

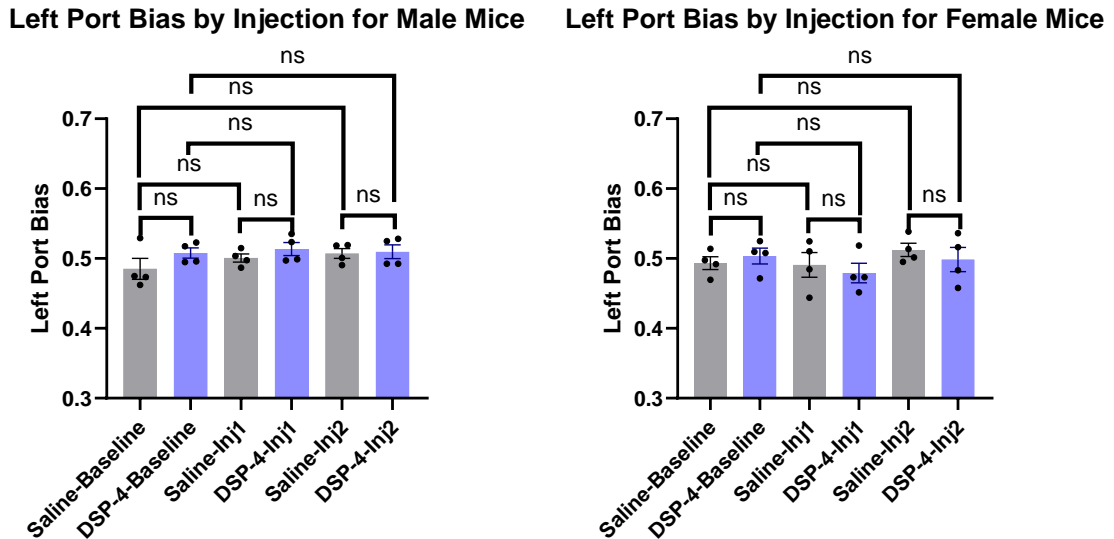


Figure 17. The probability of choosing the left port for all trials in DSP-4 and Saline injected male mice (left) during 90-10 reward probabilities compared across the baseline, first and second injections (bar = mean, error bar = SEM) (nested ANOVA $F = 1.029$, $DFn = 5$, $DFd = 18$, p -values: 0.4303). The probability of choosing the left port in DSP-4 and Saline injected female mice (right) during 90-10 reward probabilities compared across the baseline, first and second injections (bar = mean, error bar = SEM) (nested ANOVA $F = 0.6572$, $DFn = 5$, $DFd = 18$, p -values: 0.6602).

70-30

After the third injection, the water-restricted mice were placed in the behavioral box with rewards delivered asymmetrically at 70-30. The weight of the animals was measured every day the task was run and the data was calculated as the percent of each animal's original body weight. This data was compared across both DSP-4 and Saline injected mice during only the third injection condition using a nested t-test (Figure 18). Comparisons made between Saline Injection 3 – DSP4 Injection 3 were shown to be

statistically significant. However, data showing the probability of choosing the highly rewarded port, compared between Saline Injection 3 – DSP4 Injection 3 showed no statistical significance (Figure 18). The DSP4 mice appear to weigh less than the Saline mice but do not show a difference in how often they chose the highly rewarded port.

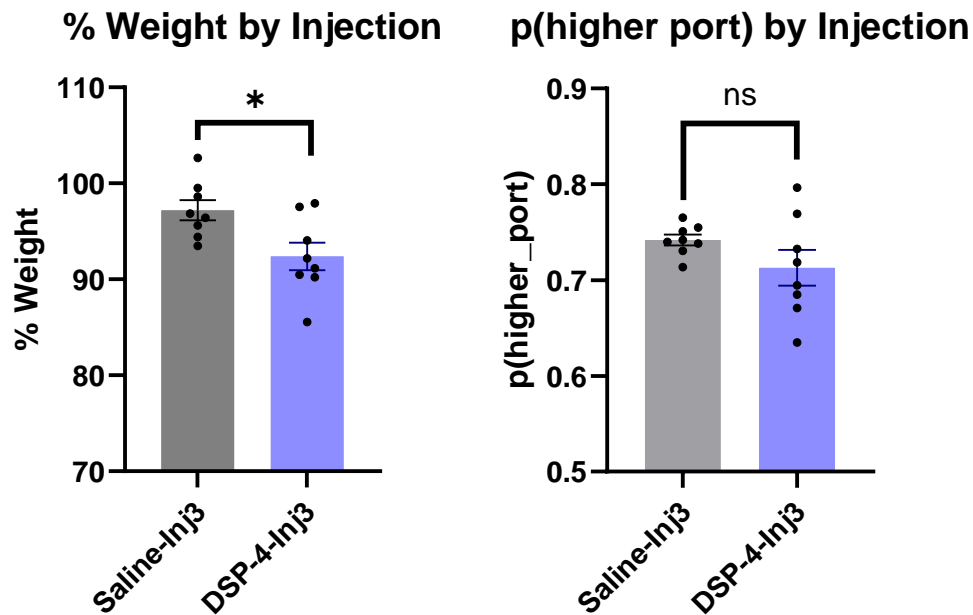


Figure 18. The average percent body weight of DSP-4 and Saline injected mice during 70-30 reward probabilities after the 3rd injection (left) (bar = mean, error bar = SEM) (nested t-test $t = 2.693$, $df = 14$, p-values: 0.0175). The probability of choosing the highly rewarding port in DSP-4 and Saline injected mice during 70-30 reward probabilities after the 3rd injection (right) (bar = mean, error bar = SEM) (nested t-test $t = 1.494$, $df = 14$, p-values: 0.1574).

The probability of choosing the highly rewarded port was also calculated during each session. This data was compared across both DSP-4 and Saline injected mice during only the third injection condition using a nested t-test (Figure 19). Comparisons made between Saline Injection 3 – DSP4 Injection 3 were shown not to be statistically significant. The data showing the probability of switching was also calculated during

these sessions, compared between Saline Injection 3 – DSP4 Injection 3, and showed no statistical significance (Figure 19).

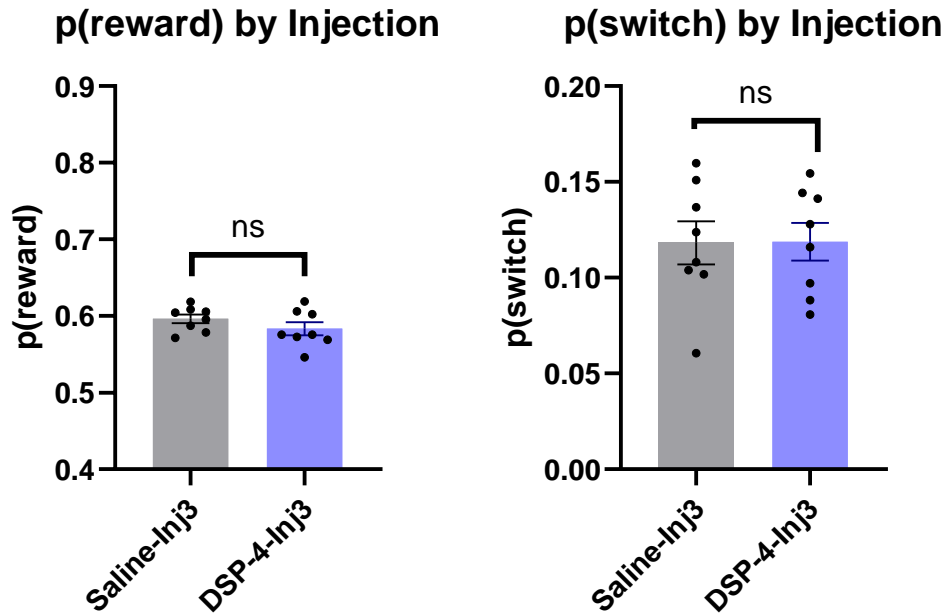


Figure 19. The probability of receiving a reward in DSP-4 and Saline injected mice during 70-30 reward probabilities after the 3rd injection (left) (bar = mean, error bar = SEM) (nested t-test $t = 1.1319$, $df = 14$, p -values: 0.2083). The probability of switching across all trials in DSP-4 and Saline injected mice during 70-30 reward probabilities after the 3rd injection (right) (bar = mean, error bar = SEM) (nested t-test $t = 0.3051$, $df = 14$, p -values: 0.9761).

The total number of trials completed was calculated during each session. This data was compared across both DSP-4 and Saline injected mice during only the third injection condition using a nested t-test (Figure 20). Comparisons made between Saline Injection 3 – DSP4 Injection 3 were shown not to be statistically significant. However, the data showing average intertrial interval was also calculated during these sessions, compared between Saline Injection 3 – DSP4 Injection 3, and showed statistical

significance (Figure 20). DSP4 injected mice appear to have longer intertrial intervals than saline injected control mice.

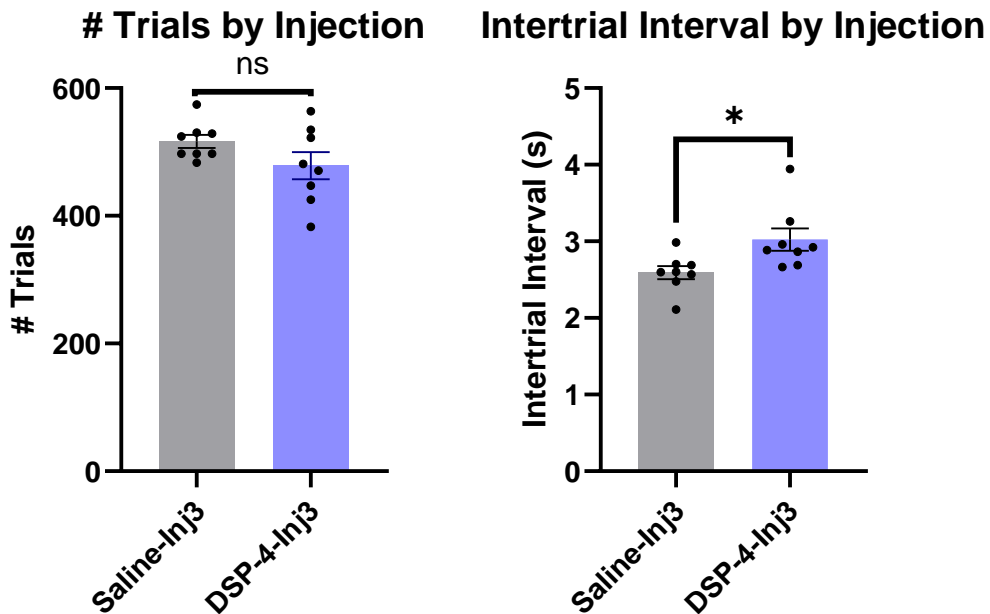


Figure 20. The average number of trials in DSP-4 and Saline injected mice during 70-30 reward probabilities after the 3rd injection (left) (bar = mean, error bar = SEM) (nested t-test $t = 1.602$, $df = 14$, p -values: 0.1314). The average intertrial interval across all trials in DSP-4 and Saline injected mice during 70-30 reward probabilities after the 3rd injection (right) (bar = mean, error bar = SEM) (nested t-test $t = 2.534$, $df = 14$, p -values: 0.0239).

The average trial duration was also calculated during each session. This data was compared across both DSP-4 and Saline injected mice during only the third injection condition using a nested t-test (Figure 21). Comparisons made between Saline Injection 3 – DSP4 Injection 3 were shown not to be statistically significant. The data showing the probability of choosing the left port was also calculated during these sessions, compared between Saline Injection 3 – DSP4 Injection 3, and showed no statistical significance (Figure 21) although there appears to be significant variance within the groups.

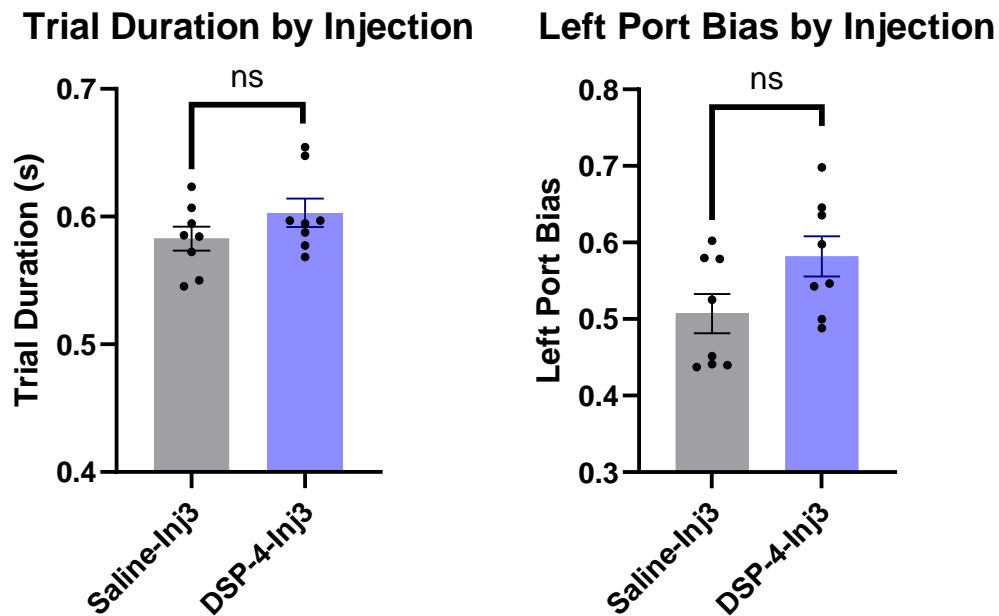


Figure 21. The average trial duration in DSP-4 and Saline injected mice during 70-30 reward probabilities after the 3rd injection (left) (bar = mean, error bar = SEM) (nested t-test $t = 1.386$, $df = 14$, p -values: 0.1876). The probability of choosing the left port across all trials in DSP-4 and Saline injected mice during 70-30 reward probabilities after the 3rd injection (right) (bar = mean, error bar = SEM) (nested t-test $t = 2.024$, $df = 14$, p -values: 0.0625).

Male vs Female 70-30

Due to the variance seen within the groups, this data was also further divided between male and female mice. The weight of the male mice was compared across both DSP-4 and Saline injected mice after the third injection condition using a nested t-test (Figure 22). Then, the weight of the female mice was compared across both DSP-4 and Saline injected mice after the third injection condition using a nested t-test (Figure 22). In the male mice, comparisons made between the Saline Injection 3 – DSP4 Injection 3 groups were statistically significant. However, in the female mice, this comparison

between the Saline Injection 3 – DSP4 Injection 3 groups did not demonstrate any statistical significance.

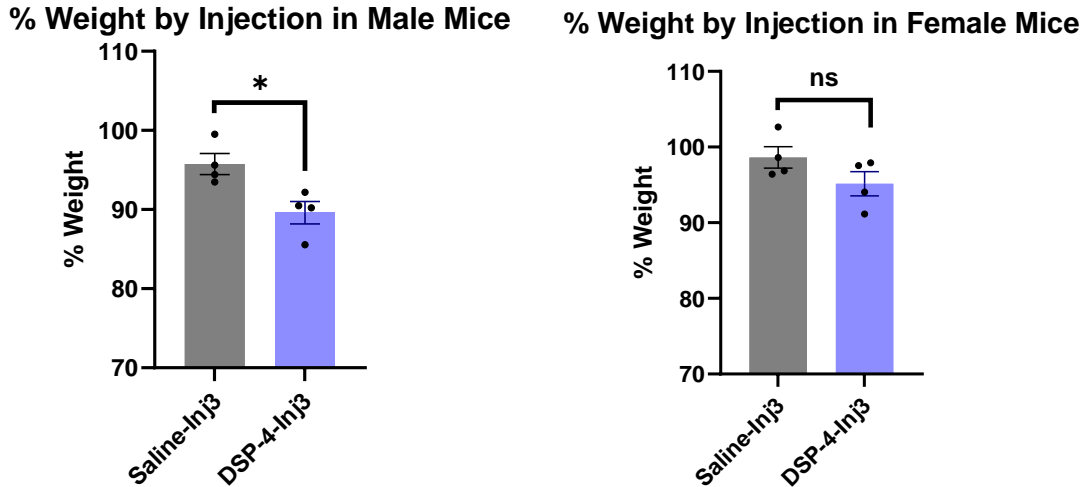


Figure 22. The average percent body weight of DSP-4 and Saline injected male mice during 70-30 reward probabilities after the 3rd injection (left) (bar = mean, error bar = SEM) (nested t-test $t = 3.160$, $df = 6$, p -values: 0.0196). The average percent body weight of DSP-4 and Saline injected female mice during 70-30 reward probabilities after the 3rd injection (right) (bar = mean, error bar = SEM) (nested t-test $t = 1.621$, $df = 6$, p -values: 0.1562).

Due to the variance seen within the groups, the data for the probability of choosing the highly rewarding port was also further divided between male and female mice. The male mice were compared across both DSP-4 and Saline injected mice after the third injection condition using a nested t-test (Figure 23). Then, the female mice were compared across both DSP-4 and Saline injected mice after the third injection condition using a nested t-test (Figure 23). In the male mice, comparisons made between the Saline Injection 3 – DSP4 Injection 3 groups were not statistically significant. In the female mice, this comparison between the Saline Injection 3 – DSP4 Injection 3 groups was also not statistically significant.

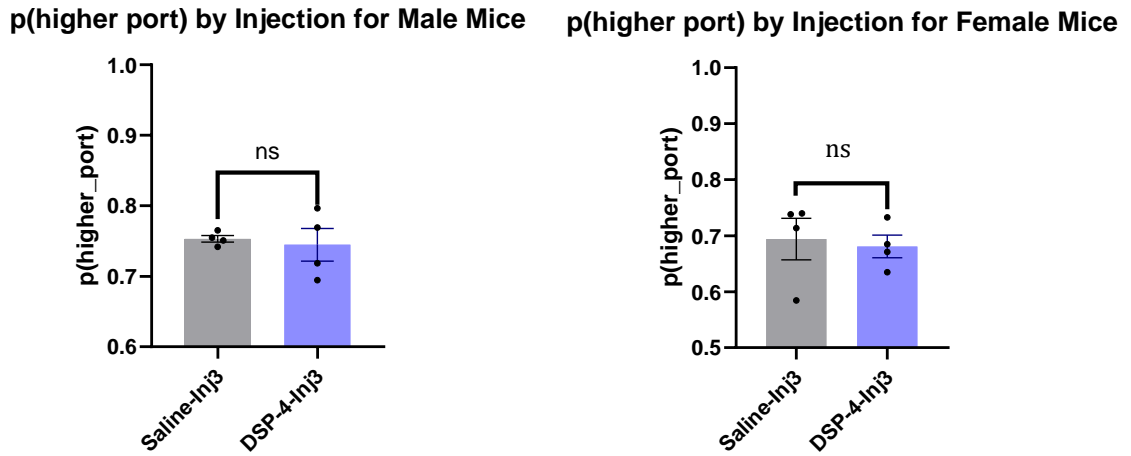


Figure 23. The probability of choosing the highly rewarding port in DSP-4 and Saline injected male mice during 70-30 reward probabilities after the 3rd injection (left) (bar = mean, error bar = SEM) (nested t-test $t = 0.3576$, $df = 6$, p-values: 0.7329). The probability of choosing the highly rewarding port in DSP-4 and Saline injected female mice during 70-30 reward probabilities after the 3rd injection (right) (bar = mean, error bar = SEM) (nested t-test $t = 0.3131$, $df = 6$, p-values: 0.7648).

Due to the variance seen within the groups, the data for the probability of receiving a reward was also further divided between male and female mice. The male mice were compared across both DSP-4 and Saline injected mice after the third injection condition using a nested t-test (Figure 24). Then, the female mice were compared across both DSP-4 and Saline injected mice after the third injection condition using a nested t-test (Figure 24). In the male mice, comparisons made between the Saline Injection 3 – DSP4 Injection 3 groups were not statistically significant. In the female mice, this comparison between the Saline Injection 3 – DSP4 Injection 3 groups was also not statistically significant.

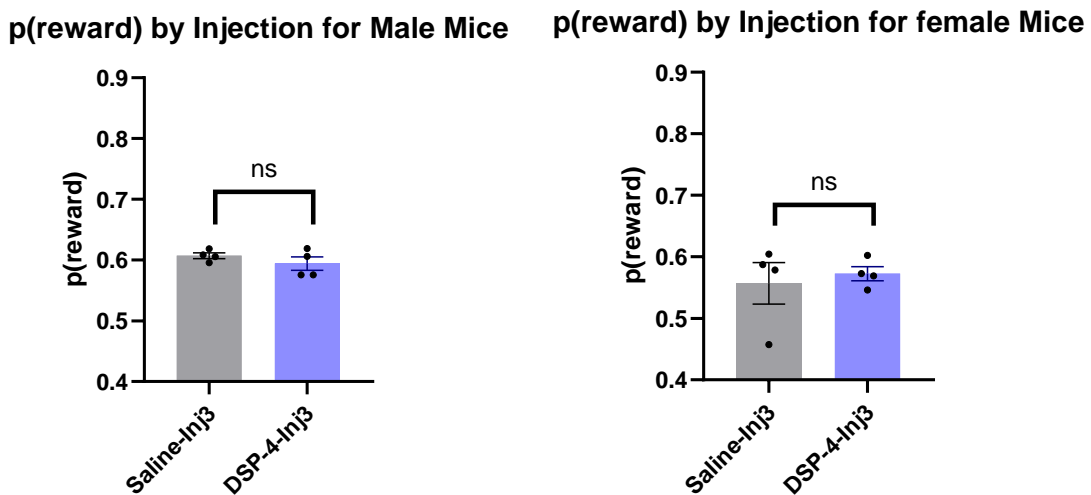


Figure 24. The probability of receiving a reward port in DSP-4 and Saline injected male mice during 70-30 reward probabilities after the 3rd injection (left) (bar = mean, error bar = SEM) (nested t-test $t = 1.083$, $df = 6$, p -values: 0.3202). The probability of receiving a reward in DSP-4 and Saline injected female mice during 70-30 reward probabilities after the 3rd injection (right) (bar = mean, error bar = SEM) (nested t-test $t = 0.4395$, $df = 6$, p -values: 0.6757).

The data for the probability of switching was also further divided between male and female mice. The male mice were compared across both DSP-4 and Saline injected mice after the third injection condition using a nested t-test (Figure 25). Then, the female mice were compared across both DSP-4 and Saline injected mice after the third injection condition using a nested t-test (Figure 25). In the male mice, comparisons made between the Saline Injection 3 – DSP4 Injection 3 groups were not statistically significant. In the female mice, this comparison between the Saline Injection 3 – DSP4 Injection 3 groups was also not statistically significant.

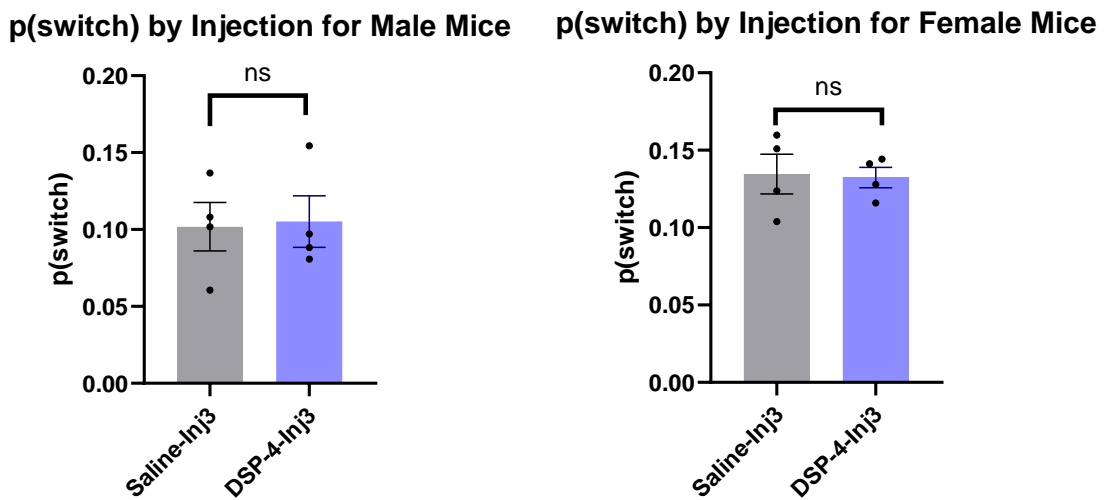


Figure 25. The probability of switching in DSP-4 and Saline injected male mice during 70-30 reward probabilities after the 3rd injection (left) (bar = mean, error bar = SEM) (nested t-test $t = 0.1443$, $df = 6$, p -values: 0.8900). The probability of switching in DSP-4 and Saline injected female mice during 70-30 reward probabilities after the 3rd injection (right) (bar = mean, error bar = SEM) (nested t-test $t = 0.2292$, $df = 6$, p -values: 0.8263).

The data for the number of trials completed each session was also further divided between male and female mice. The male mice were compared across both DSP-4 and Saline injected mice after the third injection condition using a nested t-test (Figure 26). Then, the female mice were compared across both DSP-4 and Saline injected mice after the third injection condition using a nested t-test (Figure 26). In the male mice, comparisons made between the Saline Injection 3 – DSP4 Injection 3 groups were not statistically significant. However, in the female mice, this comparison between the Saline Injection 3 – DSP4 Injection 3 groups was statistically significant. The DSP4 injected mice appear to have completed less trials than the Saline injected mice.

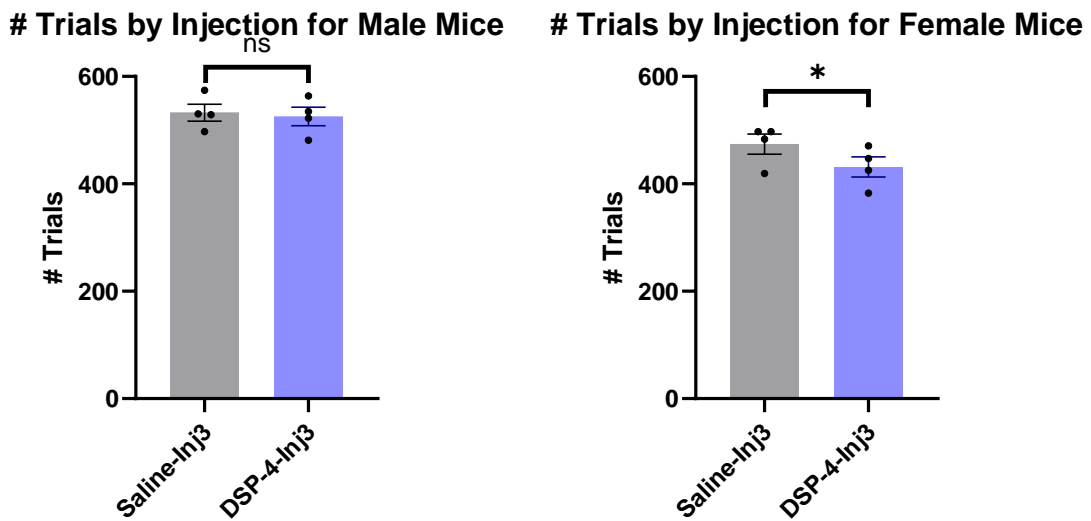
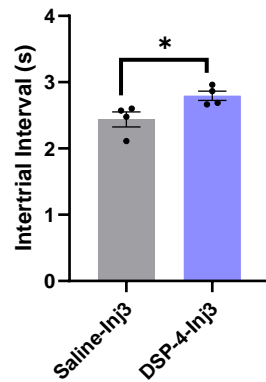


Figure 26. The average number of trials in DSP-4 and Saline injected male mice during 70-30 reward probabilities after the 3rd injection (left) (bar = mean, error bar = SEM) (nested t-test $t = 0.3112$, $df = 6$, p -values: 0.7662). The average number of trials DSP-4 and Saline injected female mice during 70-30 reward probabilities after the 3rd injection (right) (bar = mean, error bar = SEM) (nested t-test $t = 3.319$, $df = 6$, p -values: 0.0160).

The data for the average intertrial interval for each session was also further divided between male and female mice. The male mice were compared across both DSP-4 and Saline injected mice after the third injection condition using a nested t-test (Figure 27). Then, the female mice were compared across both DSP-4 and Saline injected mice after the third injection condition using a nested t-test (Figure 27). In the male mice, comparisons made between the Saline Injection 3 – DSP4 Injection 3 groups demonstrated statistical significance. The DSP4 injected mice had longer intertrial intervals than saline injected mice. However, in the female mice, this comparison between the Saline Injection 3 – DSP4 Injection 3 groups was not statistically significant.

Intertrial Interval by Injection for Male Mice



Intertrial Interval by Injection for Female Mice

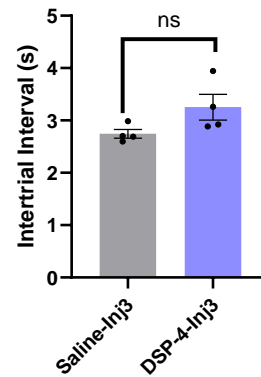
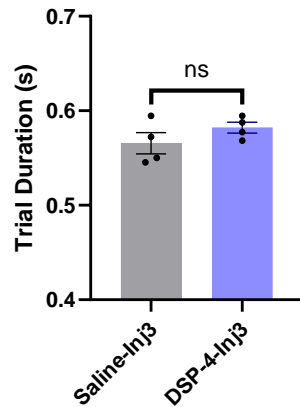


Figure 27. The average intertrial interval in DSP-4 and Saline injected male mice during 70-30 reward probabilities after the 3rd injection (left) (bar = mean, error bar = SEM) (nested t-test $t = 2.660$, $df = 6$, p -values: 0.0375). The average intertrial interval in DSP-4 and Saline injected female mice during 70-30 reward probabilities after the 3rd injection (right) (bar = mean, error bar = SEM) (nested t-test $t = 1.954$, $df = 6$, p -values: 0.0985).

The data for the average trial duration calculated during each session was also further divided between male and female mice. The male mice were compared across both DSP-4 and Saline injected mice after the third injection condition using a nested t-test (Figure 28). Then, the female mice were compared across both DSP-4 and Saline injected mice after the third injection condition using a nested t-test (Figure 28). In the male mice, comparisons made between the Saline Injection 3 – DSP4 Injection 3 groups were not statistically significant. In the female mice, this comparison between the Saline Injection 3 – DSP4 Injection 3 groups was also not statistically significant.

Trial Duration by Injection for Male Mice



Trial Duration by Injection for Female Mice

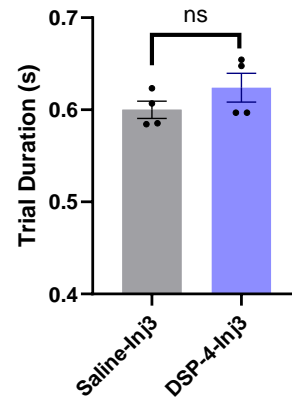
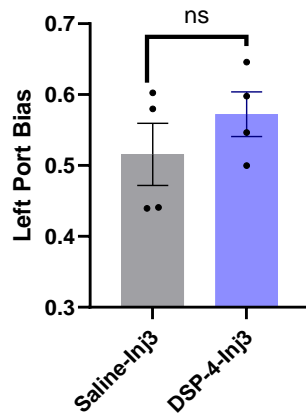


Figure 28. The average trial duration in DSP-4 and Saline injected male mice during 70-30 reward probabilities after the 3rd injection (left) (bar = mean, error bar = SEM) (nested t-test $t = 1.291$, $df = 6$, p -values: 0.2441). The average trial duration in DSP-4 and Saline injected female mice during 70-30 reward probabilities after the 3rd injection (right) (bar = mean, error bar = SEM) (nested t-test $t = 1.296$, $df = 6$, p -values: 0.2426).

The data for the probability of choosing the left port during each session was also further divided between male and female mice. The male mice were compared across both DSP-4 and Saline injected mice after the third injection condition using a nested t-test (Figure 29). Then, the female mice were compared across both DSP-4 and Saline injected mice after the third injection condition using a nested t-test (Figure 29). In the male mice, comparisons made between the Saline Injection 3 – DSP4 Injection 3 groups were not statistically significant. In the female mice, this comparison between the Saline Injection 3 – DSP4 Injection 3 groups was also not statistically significant.

Left Port Bias by Injection for Male Mice



Left Port Bias by Injection for Female Mice

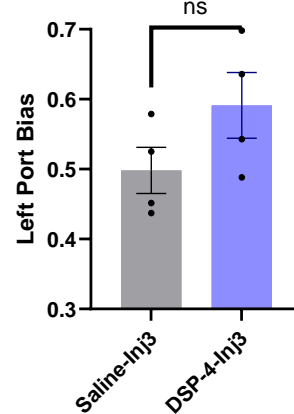


Figure 29. The probability of choosing the left port in DSP-4 and Saline injected male mice during 70-30 reward probabilities after the 3rd injection (left) (bar = mean, error bar = SEM) (nested t-test $t = 1.052$, $df = 6$, p-values: 0.3331). The probability of choosing the left port in DSP-4 and Saline injected female mice during 70-30 reward probabilities after the 3rd injection (right) (bar = mean, error bar = SEM) (nested t-test $t = 1.607$, $df = 6$, p-values: 0.1592).

Immunohistochemistry

After the end of the experiment, mice were perfused, their brains were fixed with PFA, and eventually sliced coronally and stained for NET and Tyrosine hydroxylase (TH). Sections containing the LHB and LC were scanned to compare DSP4-treated mice and saline-injected mice (Figure 30 and Figure 31). There appears to be a lack of cells and axons in the DSP4 injected mice when compared to the Saline injected mice indicating that the DSP4 injections were successful in ablating NE neurons in the mouse brain.

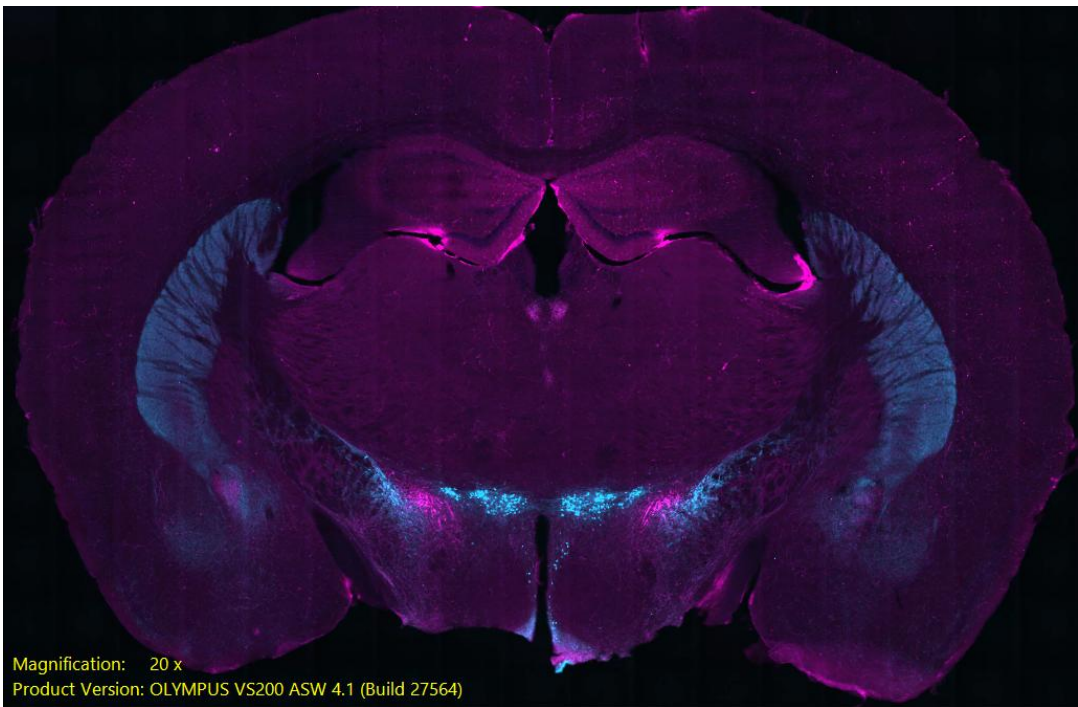
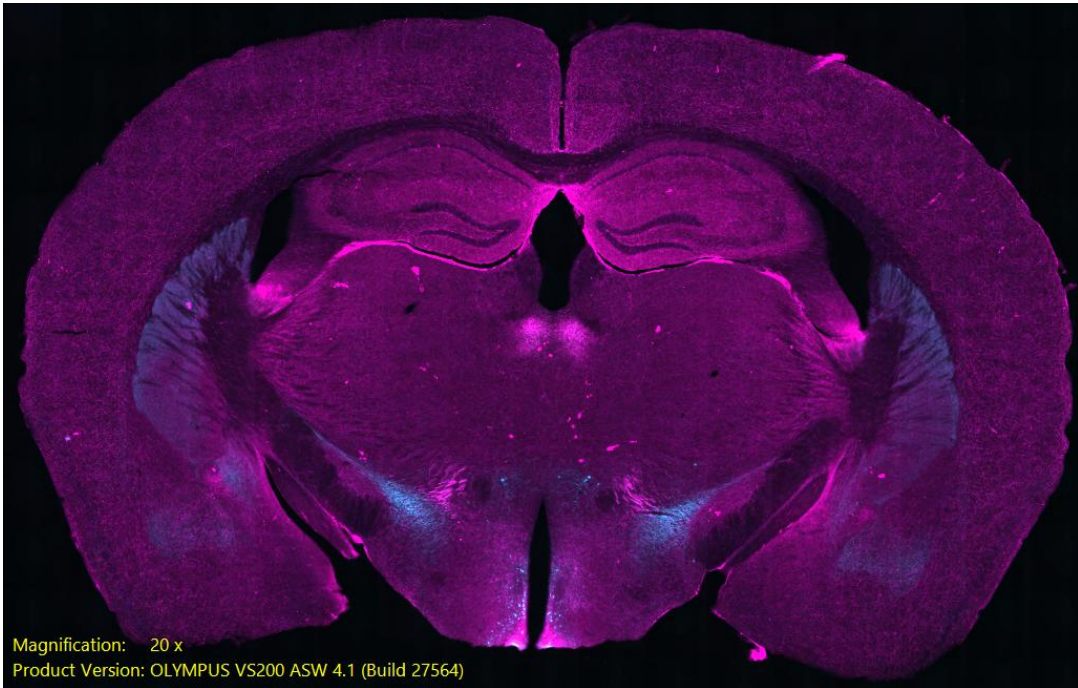


Figure 30. Representative IHC staining of coronal mouse brain sections showing the lateral habenula stained for NET and TH (Magenta = NET, Cyan = TH, Dark blue = DAPI). The top image is from a mouse injected with saline while the bottom image is from a mouse injected with DSP4.

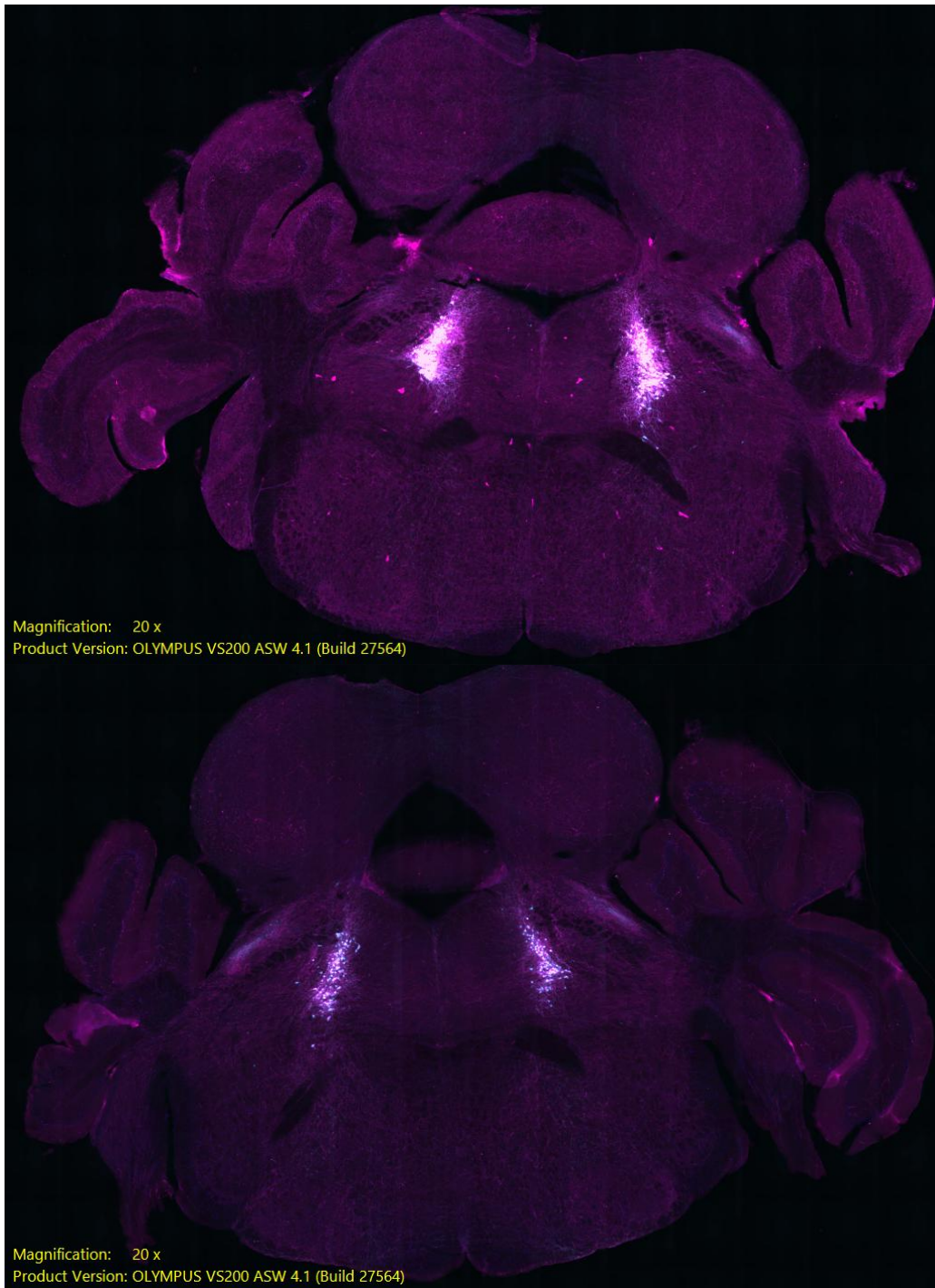


Figure 31. Representative IHC staining of coronal mouse brain sections showing the Locus Coeruleus stained for NET and TH (Magenta = NET, Cyan = TH, Dark blue = DAPI). The top image is from a mouse injected with saline while the bottom image is from a mouse injected with DSP4.

DISCUSSION

A probabilistic switching task was used in which mice rely on their history of choices and rewards to update and guide future actions (Chantranupong et al., 2023; Beron et al., 2022). It was found that mice can detect block transitions when reward probabilities switch between sides and respond by increasing the frequency of switching between reward ports. Animals also adjust their strategy based on the combination of reward probabilities within a session, as demonstrated by differences between 90/10 and 70/30 reward probability pairs. As the reward probabilities become more variable, mice integrate evidence from more past trials to inform their future decisions. When rewards become more stochastic, mice take longer to stabilize their selection of the high-reward port after a block transition, switching between ports less frequently. However, the statistical test demonstrated that there was no statistical significance in the results despite the observation of certain trends.

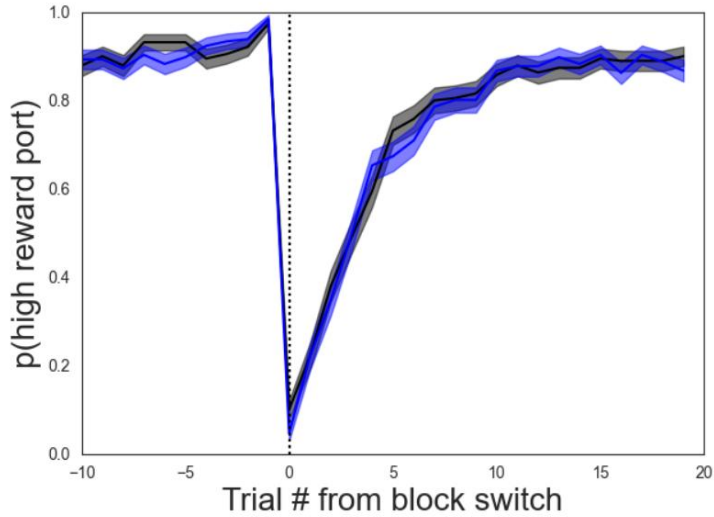
There were some significant changes in weight in both male and female mice, especially after the third injection, however, there have not been any observed changes in DSP-4 causing weight gain in rodents (Bortel 2022). There is also an increase in intertrial interval which may indicate slower movements or a lack of activity after the third injection. It is unclear if this is a sign of a lack of motivation but coupled with the weight gain and trends that indicate there is a decreased number of trials after the third injection, indicates the mice are not moving as much.

Dynamic, probabilistic switching tasks have been employed by various research groups to investigate how animals utilize their previous experiences to inform their

subsequent choices (Chantranupong et al., 2023; Beron et al., 2022; Locantore et al., 2025). In conclusion, this thesis developed an in vivo method to monitor NE interactions in the brain, particularly during decision-making, by employing a variety of tools to manipulate NE levels during a complex behavioral task. Furthermore, these findings offer a foundation for future research, enabling scientists to gain a more comprehensive understanding of the neurochemical mechanisms underlying decision-making and behavior. Further repeated studies with increased datasets would need to be conducted in order to enhance the statistical power and precision of the findings and understand the effects of norepinephrine ablation on the rodent brain.

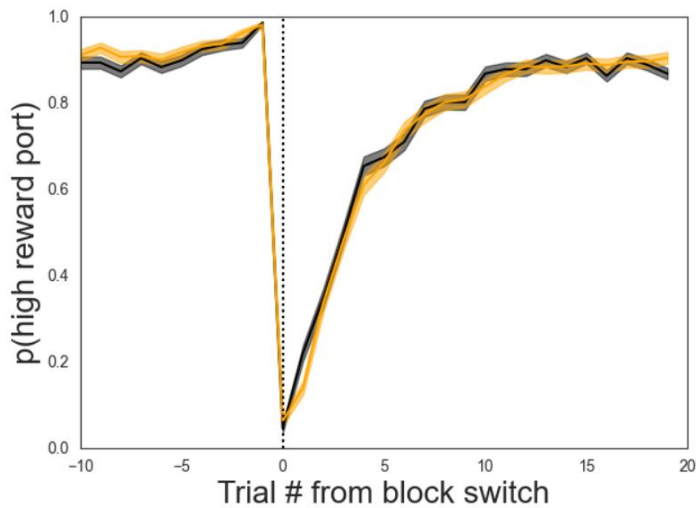
APPENDIX

probability of choosing high reward port
around the block transition



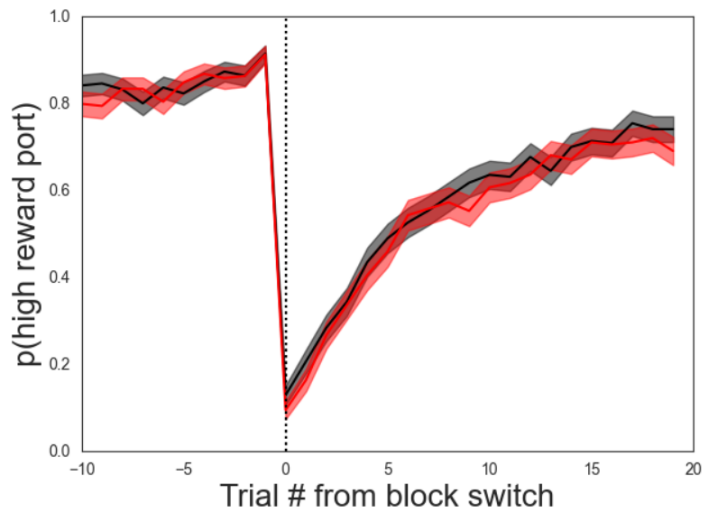
Supplemental Figure 1. The probability of choosing the highly rewarding port around a block transition after injection 1 at 90-10 probabilities (grey = saline injected mice, blue = dsp4 injected mice).

probability of choosing high reward port
around the block transition



Supplemental Figure 2. The probability of choosing the highly rewarding port around a block transition after injection 2 at 90-10 probabilities (grey = saline injected mice, orange = dsp4 injected mice).

probability of choosing high reward port
around the block transition



Supplemental Figure 3. The probability of choosing the highly rewarding port around a block transition after injection 3 at 70-30 probabilities (grey = saline injected mice, red = dsp4 injected mice).

BIBLIOGRAPHY

- Baker, P. M., Jhou, T., Li, B., Matsumoto, M., Mizumori, S. J. Y., Stephenson-Jones, M., & Vicentic, A. (2016). The lateral habenula circuitry: Reward processing and cognitive control. *The Journal of Neuroscience*, *36*(45), 11482–11488. <https://doi.org/10.1523/jneurosci.2350-16.2016>
- Beron, C. C., Neufeld, S. Q., Linderman, S. W., & Sabatini, B. L. (2022). Mice exhibit stochastic and efficient action switching during probabilistic decision making. *Proceedings of the National Academy of Sciences*, *119*(15). doi:10.1073/pnas.2113961119
- Berridge, C. W., & Waterhouse, B. D. (2003). The locus coeruleus–noradrenergic system: Modulation of Behavioral State and state-dependent cognitive processes. *Brain Research Reviews*, *42*(1), 33–84. doi:10.1016/s0165-0173(03)00143-7
- Bortel, A. (2022). Nature of DSP-4-induced neurotoxicity. *Handbook of Neurotoxicity*, 669–690. https://doi.org/10.1007/978-3-031-15080-7_75
- Breton-Provencher, V., Drummond, G. T., & Sur, M. (2021). Locus coeruleus norepinephrine in learned behavior: Anatomical modularity and spatiotemporal integration in targets. *Frontiers in Neural Circuits*, *15*. doi:10.3389/fncir.2021.638007
- Bromek, E., Danek, P. J., Wójcikowski, J., Basińska-Ziobroń, A., Pukło, R., Solich, J., Dziedzicka-Wasylewska, M., & Daniel, W. A. (2022). The impact of noradrenergic neurotoxin DSP-4 and noradrenaline transporter knockout (net-KO) on the activity of liver cytochrome P450 3A (CYP3A) in male and female mice. *Pharmacological Reports*, *74*(5), 1107–1114. <https://doi.org/10.1007/s43440-022-00406-8>
- Chandler, D. J., Jensen, P., McCall, J. G., Pickering, A. E., Schwarz, L. A., & Totah, N. K. (2019). Redefining noradrenergic neuromodulation of behavior: Impacts of a modular locus coeruleus architecture. *The Journal of Neuroscience*, *39*(42), 8239–8249. <https://doi.org/10.1523/jneurosci.1164-19.2019>
- Chantranupong, L., Beron, C. C., Zimmer, J. A., Wen, M. J., Wang, W., & Sabatini, B. L. (2023). Dopamine and glutamate regulate striatal acetylcholine in decision-making. *Nature*, *621*, 577–585. doi:10.1038/s41586-023-06492-9
- Gannon, M., Che, P., Chen, Y., Jiao, K., Roberson, E. D., & Wang, Q. (2015). Noradrenergic dysfunction in alzheimer’s disease. *Frontiers in Neuroscience*, *9*. doi:10.3389/fnins.2015.00220

- Hikosaka, O., Sesack, S. R., Lecourtier, L., & Shepard, P. D. (2008). Habenula: Crossroad between the basal ganglia and the limbic system. *The Journal of Neuroscience*, 28(46), 11825–11829. <https://doi.org/10.1523/jneurosci.3463-08.2008>
- Locantore, J., Liu, Y., White, J., Wallace, J. B., Beron, C., Kraft, E., Sabatini, B.; Wallace, M. (2025). Mixed representations of choice direction and outcome by GABA/glutamate cotransmitting neurons in the entopeduncular nucleus. *eLife*, 13. doi:10.7554/elife.100488.3
- Mandela, P., & Ordway, G. A. (2006). The norepinephrine transporter and its regulation. *Journal of Neurochemistry*, 97(2), 310–333. doi:10.1111/j.1471-4159.2006.03717.x
- Mondoloni, S., Mameli, M., & Congiu, M. (2022). Reward and aversion encoding in the lateral habenula for innate and learned behaviours. *Translational Psychiatry*, 12(1). <https://doi.org/10.1038/s41398-021-01774-0>
- Palkovits, M., & Brownstein, M. J. (1983). Locus Coeruleus. In *Advances in Cellular Neurobiology* (Vol. 4, pp. 81–103). Elsevier. Retrieved from <https://www.sciencedirect.com/science/article/abs/pii/B9780120083046500087>.
- Poe, G. R., Foote, S., Eschenko, O., Johansen, J. P., Bouret, S., Aston-Jones, G., et al. (2020). Locus Coeruleus: A new look at the Blue Spot. *Nature Reviews Neuroscience*, 21(11), 644–659. doi:10.1038/s41583-020-0360-9.
- Sara, S. J. (2009). The locus coeruleus and noradrenergic modulation of cognition. *Nature Reviews Neuroscience*, 10(3), 211–223. doi:10.1038/nrn2573
- Stephenson-Jones, M., Yu, K., Ahrens, S., Tucciarone, J. M., van Huijstee, A. N., Mejia, L. A., Penzo, M. A., Tai, L.-H., Wilbrecht, L., & Li, B. (2016). A basal ganglia circuit for evaluating action outcomes. *Nature*, 539(7628), 289–293. <https://doi.org/10.1038/nature19845>
- Tabansky, I., Liang, Y., Frankfurt, M., Daniels, M. A., Harrigan, M., Stern, S., ... Pfaff, D. W. (2018). Molecular profiling of reticular gigantocellularis neurons indicates that enos modulates environmentally dependent levels of arousal. *Proceedings of the National Academy of Sciences*, 115(29). doi:10.1073/pnas.1806123115
- Tortorelli, L. S., Garad, M., Megemont, M., Haga-Yamanaka, S., Goel, A., & Yang, H. (2022). Variations of neuronal properties in the region of Locus Coeruleus Of Mice. *Brain Research*, 1845. <https://doi.org/10.1101/2022.08.19.504582>
- Wallace, M. L., Huang, K. W., Hochbaum, D., Hyun, M., Radeljic, G., & Sabatini, B. L. (2020). Anatomical and single-cell transcriptional profiling of the murine habenular complex. *eLife*, 9. <https://doi.org/10.7554/elife.51271>

Zhong, H., & Minneman, K. P. (1999). A1-adrenoceptor subtypes. *European Journal of Pharmacology*, 375(1–3), 261–276. [https://doi.org/10.1016/s0014-2999\(99\)00222-8](https://doi.org/10.1016/s0014-2999(99)00222-8)

CURRICULUM VITAE

